Chapter 2

Chronology of Pluton Emplacement and Regional Deformation in the Southern Sierra Nevada Batholith, California

Saleeby, J.B., Division of Geological and Planetary Sciences, California Institute of Technology, Pasadena CA 91125
Ducea, M., Department of Geosciences, University of Arizona, Tucson AZ
Busby, C., Department of Geosciences, University of California, Santa Barbara
Nadin, E.S., Division of Geological and Planetary Sciences, California Institute of Technology, Pasadena CA 91125
Wetmore, P.H., Department of Geology, University of South Florida, Tampa, FL 33620

Abstract

Cretaceous plutonic rocks of the southern Sierra Nevada batholith (SNB) between latitudes 35.5º N and 37˚ N preserve an oblique crustal section through the southern SNB. Prior studies have produced large U/Pb zircon data sets for an aerially extensive region of the batholith north of this area, and for the lower crustal rocks to the south. We present a large set of new U/Pb zircon age data that tie together the temporal relations of pluton emplacement and intra-arc ductile deformation for the region. We define five informal intrusive suites in the area based on petrography, structural setting, U/Pb zircon ages and patterns in initial $^{87}Sr/^{86}Sr$. Two regionally extensive suites, the ca. 105-98 Ma Bear Valley and ca. 93-84 Ma Domelands, underlie the entire southwestern and eastern regions of the study area, respectively, and extend beyond the limits of the study area. A third regionally extensive suite (the ca. 100-96 Ma Needles suite) cuts out the northern end of the Bear Valley suite and extends for an unknown distance to the north of the study area.

The Bear Valley and Needles suites are tectonically separated from the Domelands suite by the proto-Kern Canyon fault (PKCF), a regional Late Cretaceous ductile shear zone that runs along the axis of the southern SNB. The ca. 105-102 Ma Kern River suite also lies west of the PKCF, and constitutes the sub-volcanic plutonic complex for the ca. 105-102 Ma Erskine Canyon sequence, a ≥2 km thick silicic ignimbrite-hypabyssal complex. The ca. 100-94 Ma South Fork suite lies east of the PKCF. It records temporal and structural relations of high-magnitude ductile strain and migmatization in its host metamorphic pendant rocks commensurate with its magmatic emplacement.

Integration of the U/Pb age data with structural and isotopic data provides insight into the chronology and kinematics of regional intra-arc ductile deformation, indicating that east-side-up reverse sense ductile shear along the PKCF may have started as early as ca. 100 Ma, and was clearly operating by ca. 94 Ma. Dextral sense ductile shearing including a small reverse component commenced at ca. 94 Ma and was in its waning phases by ca. 83 Ma. Because ~50 percent of the southern SNB was magmatically emplaced during this time interval, primarily within the east wall of the PKCF, the shear zone's total dextral slip history is only loosely constrained. The changing kinematic patterns recorded in the age and structural relations of the principal damage zone of the PKCF are consistent with age and deformational relations of ductile shear zones present within the shallow-level central SNB, and with those of the deep-level exposures in the southernmost SNB. This deformational regime correlates with flat slab segment subduction beneath the southern California region batholithic belt, and the resulting tilting and unroofing of the southern SNB oblique crustal section. These events may be correlated to the onset of the Laramide orogeny.

Introduction

The SNB is perhaps the most intensively studied batholithic belt in the world (cf. Evernder and Kistler, 1972; Bateman, 1983; Saleeby, 1990; Coleman and Glazner, 1997; Ducea and Saleeby, 1998; Ducea, 2001; Sisson et al., 1996). This sparse sampling of SNB references reflects a few of the many topical and synthesis-type papers that have been published. These have benefited from, and to a great extent were made possible by, systematic quadrangle mapping by the U.S. Geological Survey between latitudes 36.25° N and 38.25°N. Such field mapping facilitated a later generation of intensive regional efforts in geochronology and igneous barometric determinations of pluton emplacement depths, which are discussed in depth below. These studies have in turn facilitated the pursuit of fundamental questions concerning batholith belt structure and petrogenesis.

Regional geochronological studies indicate that batholithic magmatism initiated in the Sierra Nevada as early as ca. 248 Ma, continued semi-continuously through much of the Mesozoic, and culminated with its highest volume production in the ca. 100-85 Ma time interval (Evernden and Kistler, 1972; Saleeby and Sharp, 1979; Stern el al., 1981; Saleeby et al., 1987; Chen and Moore, 1982; Coleman et al., 2004; Saleeby and Dunne, 2006). These studies show clear temporal and spatial patters in the loci of magmatism expressed most clearly by a general west to east migration of pluton emplacement through the Cretaceous. Superimposed on this longitudinal age zonation pattern is an along-strike depth of exposure gradient whereby regionally continuous shallow-level batholithic rocks (<10 km emplacement depths) grade continuously into deep-level exposures (~35 km) of the Tehachapi complex at the southern end of the range (Ague and

Brimhall, 1987; Pickett and Saleeby, 1993; Ague, 1997; Nadin, Chapter 3). Up to this point, extensive U/Pb zircon geochronological data sets have existed for a large area of the shallow-level exposures to the north of the study area (Saleeby and Sharp, 1980; Stern et al., 1981; Chen and Moore, 1982; Saleeby et al., 1980; Tobisch et al., 1995; Coleman et al., 2004), and also the Tehachapi complex to the south (Saleeby et al., 1987; 2006; Pickett and Saleeby, 1994). However, in the area of the steepest longitudinal depth of exposure gradient, a critical data gap has existed. In this paper we fill this gap.

The U/Pb zircon data presented in this paper are tied to regional and detailed mapping, thus facilitating a number of important tectonic and petrogenetic pursuits. We may now track pluton emplacement patterns in time and space over nearly a complete sialic crustal column interval, as well as study the temporal patterns of deformation along a whole-crust penetrating shear/fault zone. The strategy employed in this study follows two major tacks. First, high precision U/Pb zircon ages were determined by isotope dilution procedures on multiple zircon fractions commensurate with a decadal effort in systematic and topical mapping along an ~ 30 km wide corridor of the axial SNB between latitudes 35º N and 36.1º N. The structural and geochronological relations established by this effort were then complemented by a recent regional-scale effort in zircon geochronology utilizing laser ablation ICP mass spectrometric techniques. This rapid analytical technique has facilitated a regional-scale consolidation of structural and age relations established in the first tack. In the text below, we give an overview of the major tectonic and petrogenetic features of the southern SNB from a geochronological perspective, present a detailed discussion of our new data, and finally focus on several key issues in batholith tectonics and petrogenesis.

Map relations and nomenclature

Mapping efforts in the study area have consisted of our own regional and detailed topical studies, and regional-scale mapping of Ross (1989; 1995). The detailed topical studies have focused on the PKCF and proximal plutons, and on a number of metamorphic pendants and their hosting plutons. The work of Ross has been instrumental in the designation of major plutonic units based primarily on field petrography and intrusive relations. We adopt and modify the regional pluton nomenclature developed by Saleeby et al. (1987) for the Tehachapi complex, and subsequently extended northward through the study area and added upon by Ross (1989, 1995). Rocks of the study area may to a first order be broken into Paleozoic-Mesozoic metamorphic pendants and Cretaceous batholithic rocks. Early Mesozoic members of the SNB have been resolved south of latitude 36.4º N only in the extreme southeastern Sierra (Fig. 1) east of the Kern Plateau shear zone (Dunne and Saleeby, 1993, 2006). Early Mesozoic members of the SNB are notably lacking in the study area. Below we briefly discuss the framework pendants of the study area, and the batholithic units for which we report U/Pb zircon age data.

Metamorphic Pendants

Metamorphic pendant rocks of the study area are described in detail in Chapter 4, but will be cursorily introduced here. These rocks were named the Kernville series by Miller and Webb (1940), and metasedimentary rocks of Long Canyon, Fairview, and the Keene-Tehachapi belt by Ross (1989, 1995). These consist of high-grade quartzite,

marble, psammitic and pelitic schist and subordinate mafic and silicic metavolcanic rocks. They were grouped into the Kings sequence by Saleeby et al. (1978) and Saleeby and Busby (1996), and correlated primarily to Upper Triassic – Lower Jurassic pendants extending northward from the study area to at least 38˚ N (Bateman and Clark, 1974). All direct dates on the Kings sequence are of early Mesozoic age. The pendant rocks of the study area are near-pervasive high-strain tectonites. Those dispersed along the PKCF consist both of incompletely annealed fault rocks with variable brittle overprints and strongly annealed high-magnitude strain metamorphic tectonites (Busby-Spera and Saleeby, 1990; Saleeby and Busby, 1996; Chapter 4). Those pendants lying outside the PKCF are typically high-strain annealed rocks as well, with ductile deformation fabrics recording synplutonic deformation commensurate with peak metamorphic equilibration (Saleeby and Busby, 1986; Saleeby and Zeng, 2006). The age data presented here better constrain the timing of deformation recorded in the pendants. The pattern of high-strain thermal metamorphism pervading the pendant rocks, including those outside the PKCF, has one important exception. A domain of relatively low pluton emplacement depths occurs west of the PKCF between latitudes ~35.5˚ N and ~35.9˚ N (Fig. 1). This domain corresponds primarily to the area underlain by the Intrusive Suite of the Kern River, interpreted as a subvolcanic intrusive complex. Thermal metamorphism in the pendant rocks of this domain involved primarily the development of hornfelsic textures with relatively low levels of attendant strain, and thus protolith and pre-batholithic deformational features are well preserved. As deeper crustal levels are traversed southwards from this shallow-level domain, the thermal overprint recorded in the pendant rocks exhibits progressively more attendant ductile strain, which at its extreme renders

anatectic migmatites. Metamorphic pendants of the study area that lie along the PKCF between latitudes 35.46˚ N and 35.83˚ N include an unconformable infold and related hypabyssal intrusions, as well as transposed lenses within the PKCF of felsic volcanic and hypabyssal rocks (Saleeby and Busby-Spera, 1986). Based on our detailed mapping, petrography and zircon age data, the volcanogenic rocks can for the most part be separated from the underlying rocks, and are shown to be of mid-Cretaceous age. The mid-Cretaceous rocks are informally named the Erskine Canyon sequence based on a well-preserved section where the basal unconformity is preserved in Erskine Canyon (Fig. 3). The Erskine Canyon sequence is shown below to be closely related to shallow-level plutons of the Kern River intrusive suite.

Intrusive Units

We have grouped most plutons of the study area into five informal intrusive suites (Table 1; Fig. 2). Two of the suites are regionally extensive – underlying an area of ~100x50 km – and consist of numerous bodies emplaced incrementally over ~5-10 m.y. time intervals. These two intrusive suites are completely separated by the PKCF, with the Bear Valley suite to the west (after Saleeby et al., 1987), and the Domelands suite to the east (modified after Ross, 1989, 1994).

The Bear Valley suite is predominantly tonalitic with subordinate gabbroids and granodiorite. It was originally defined in the deep-level exposures south of the study area. The dominant rock type, Tonalite of Bear Valley Springs, is shown to extend from ~8 kb level exposures in the south continuously for over ~ 60 km northward into the study area where it is exposed as shallow as ~2 kb levels. It is in general bounded to the

north by additional shallower-level units of the Bear Valley suite, including the Granodiorite of Poso Flat and the Tonalite of Mount Adalaide. The bulk of the Bear Valley suite was intruded over the ca. 98-102 Ma time interval, although members of the suite in the western domains of the Tehachapi complex were intruded as far back as ca. 105 Ma (Pickett and Saleeby, 1994). Throughout its length, the Bear Valley suite contains numerous synplutonic enclaves and commingled dikes of gabbro and diorite, as well as local enclaves of Early Cretaceous (ca. 120 – 108 Ma) tonalitic intrusions. The entire known north-south extent of the Bear Valley suite is ~120 km. It is at least 50 km in east-west extent, bounded to the east by the PKCF and extending well out into the San Joaquin Valley subsurface (Ross, 1994).

The Domelands intrusive suite is predominantly granitic-granodioritic in composition. Mafic granodiorite enclaves on the scale of 1-3 km, derived from South Fork suite intrusives, are widespread in the Domelands suite. This suite is named after the Domelands Wilderness Area situated in the northeast quadrant of the study area. The Domelands suite was intruded primarily over the ca. 87-93 Ma time interval, although local intrusive sheets and dikes as old as ca. 95 Ma and as young as 83 Ma are also included in it.

Additional clusters of apparently consanguineous plutons are grouped into three less extensive suites. Plutons that resemble parts of the Bear Valley suite (Table 1, Fig. 2) but are isotopically distinct and of more limited compositional range (Saleeby et al., 1987, Kistler and Ross, 1990; Pickett and Saleeby, 1993) have been grouped into the Needles intrusive suite. This suite appears to underlie an extensive area to the north of and on strike with the Bear Valley suite, extending for an unknown distance beyond the

limits of the study area. The Needles suite is also distinguished from the Bear Valley suite by its younger spread of igneous ages (ca. 95-100 Ma). Two less extensive intrusive suites are defined in the Lake Isabella – Kernville region (Fig. 2). These are completely separated by the PKCF. The Kern River suite is a distinct shallow-level intrusive complex characterized primarily by veri-textured granite-granodiorite with commingled mafic dike rock. Structural position and age range (ca. 102-105 Ma) suggest that this suite is the sub-volcanic intrusive complex for the Erskine Canyon volcanic sequence. In addition to its slightly older age range, the Kern River suite is distinguished from the Bear Valley suite by its distinctly more felsic composition, its distinctly shallower-level character, its spatial and temporal association with the Erskine Canyon volcanic sequence, and its distinctly higher range of Sr_i. The South Fork intrusive suite is a distinct cluster of small, mainly mafic granodiorite and diorite plutons that lie east of the PKCF in the Lake Isabella – South Fork Valley area (Fig. 2). It was emplaced over the 100-94 Ma time interval at distinctly deeper crustal levels (4-5 km) than the Kern River suite immediately west of the PKCF (Nadin, Chapter 3). The South Fork suite is also distinct in that during its emplacement the Kings sequence host rocks underwent pervasive high-magnitude ductile strain and extensive partial melting along relatively broad high-grade aureoles (Saleeby and Busby-Spera, 1986; Zeng et al., 2005, 2006; Saleeby and Zeng, 2006). Enclaves of South Fork suite rocks are transposed along with high-grade pendant rocks within the eastern margin of the PKCF, and also occur as widely dispersed enclaves within high-volume granitoids of the Domelands suite. Numerous smaller plutonic units occur in the study area, but are not differentiated in Figure 2. Many of them have compositional and textural features and contact relations

suggesting that they have affinities to the major intrusive suites defined above. Except for a series of small plutons belonging to the South Fork suite, studied in detail by Saleeby and Zeng (2006), direct igneous age constraints are lacking for these smaller plutons.

U/Pb zircon data

We present new U/Pb zircon age data for 49 samples of major plutonic units and associated dikes that bear critical structural relations. Data collection was undertaken both on regional and detailed scales in order to establish intrusive and deformational chronologies. The detailed aspects encompass close integration with structural analysis of the PKCF, while the regional scale was applied to aerially extensive plutonic units. Our U/Pb zircon data consist of both conventional TIMS isotope dilution measurements on multiple fractions of small highly purified populations, and laser ablation ICP-MS analyses on populations of single grains. Tabulated isotopic data and a description of the analytical techniques used are presented in Appendix 1.

The zircon age data is in general covered by an oldest to youngest suite and intra-suite pluton emplacement progression, and are discussed in their geologic context. The igneous age assignments are presented in Table 1 along with critical information on sample location, petrography, and available Sr_i. Where the Sr_i data are shown as a range of values, the ranges reflect multiple determinations on numerous samples proximal to the zircon sample location.

Intrusive Suite of the Kern River

Intrusive units of this suite for which U/Pb zircon are presented includes the Granite of Kern River, Granite of Portuguese Pass, Granite of Bodfish Canyon, Granite of Baker Point, and mafic intrusives that are commingled with the Granite of Saddle Springs Road (Fig. 2). The latter unit appears to be a complex of mafic veri-textured intrusives that were commingled with granitic rocks of Bodfish Canyon affinity. These units all have characteristics of shallow-level igneous emplacement (Nadin, Chapter 3), and the age data presented here along with the structural setting indicate that this suite was the sub-volcanic intrusive complex of the Erskine Canyon sequence.

The Granite of Kern River is the most voluminous intrusive body of this suite. It is a composite body with generally subtle internal contacts marked by textural variations, and locally accented by commingled mafic dikes and inclusion clusters. It is cut internally by a series of hypabyssal-textured dikes named the Granite of Baker Point. Along its eastern to northern margins the Kern River granite cuts sharply across structures within the bounding Fairview pendant (Fig. 2; Nadin, Chapter 5). North of the Yellowjacket Ridge volcanic neck its commingled marginal zone extends in a shallow east-dipping sill-like fashion into the pendant as though it were "stacked in" beneath the Yellowjacket Ridge body (Fig. 2). In the Erskine Canyon area lenticular apophyses of both Kern River and Bodfish Canyon granite extend concordantly into the Kings sequence-Erskine Canyon sequence as very thick, sill-like bodies (Fig.3). We present new zircon age data for four phases of the main Kern River granite body, and for a deformed lens that lies within the PKCF (samples K1-K5). Samples K1 and K2 are from the main body west of the KCF. They yield externally concordant ages of 105.0±0.3 Ma

and 104.3±0.5 Ma, respectively (Fig. 4). Samples K3 and K4 are from east of the KCF. They yield U/Pb age frequency spectra indicating ages of 104.0±1.8 Ma and 106.5±3.4 Ma, respectively (Fig. 6). Sample K5 yields a U/Pb spectrum with considerable scatter about a 106.5±3.4 Ma mean. Scatter here could represent the effects of minor disturbance of some grains in response to high-temperature ductile deformation within the PKCF.

Additional distinctive granitic plutons of the Kern River suite include the Granite of Portuguese Pass (sample K6) and the Granite of Bodfish Canyon (K7). Both of these plutons are compositionally similar to the Kern River granite, but they typically lack the distinctive porphyritic textures of the latter. The Portuguese Pass pluton is separated from the Granite of Kern River by a narrow pendant, and is otherwise surrounded by northernmost Bear Valley and Needles suite plutons (Fig. 2). The Bodfish Canyon pluton is encased in pendant rocks except to the south where it grades into the Granite of Saddle Springs Road. Sample K6 yielded a sparse fine-grained zircon population with an internally concordant age of 103.2± 0.8 Ma (Fig. 4). Sample K7 yielded a discordant array of fractions dispersing upwards from a lower intercept of 102.8± 0.5 Ma, and projecting to an upper intercept of 1916±160 Ma (Fig. 5). The lower intercept is interpreted as the igneous emplacement age. The Granite of Saddle Springs Road appears to be the southward continuation of the Bodfish Canyon pluton, but with abundant commingled mafic intrusions and inclusion swarms. Sample K8 is from a commingled dioritic mass. Its fine fraction yields an internal concordant age, while its coarser two fractions are slightly discordant (Fig. 4). The discordant fractions lift slightly off of Concordia suggestive of minor inheritance of substantially older, Proterozoic (?)

zircon. The internally concordant fraction age of 102.5±0.5 Ma is interpreted as the igneous age of the commingled mafic rock, which is consistent with the 102.8±0.5 Ma age determined for the Bodfish Canyon granite with which it appears to be commingled.

The largest known texturally homogeneous body of the Baker Point composite granitic dike(s) was sampled adjacent to where it is observed to intrude the Kern River granite (sample K9). The rock in this location is dacite porphyry. This sample yielded an externally concordant age of 102.6±0.5 Ma (Fig. 4). The texture of this sample is transitional between the distinctly porphryritic-fine groundmass phases of the Kern River granite and textures observed in the Erskine Canyon sequence hypabyssal intrusions. The Baker Point dikes are interpreted as consanguineous with the hypabyssal intrusions.

Samples studied here from Kern River intrusive suite, like those of the Erskine Canyon sequence, cluster between ca. 105 and 102 Ma in age. Initial strontium isotopic data presented in Kistler and Ross (1990) support the petrogenetic affinity of the Erskine Canyon sequence and the Kern River intrusive suite, whose values overlap and are distinct from all other values presented for rocks west of the PKCF. These relations, in conjunction with structural position and textural relations, indicate that the Kern River suite is part of the high-level sub-volcanic intrusive complex of the Erskine Canyon sequence.

Intrusive Suite of Bear Valley

The Bear Valley suite was originally defined as a suite of gabbroic to tonalitic intrusives of ca. 102-98 Ma age within the Tehachapi complex, and was later extended to include intrusives of ca.105 Ma age further to the west in the western Tehachapi range

(Saleeby et al., 1987; Pickett and Saleeby, 1994). Regional mapping extends the principal plutonic units of this suite northward to ~35.75°N (Ross, 1989, 1994; this study). The principal units of the suite that extend northward into the study area are the Tonalite of Bear Valley Springs and the Tonalite of Mount Adelaide (Fig. 2). Based on petrographic similarities, continuity in compositional variations, structural position, age data presented here, and Sr_i, the Granodiorite of Poso Flat is included in the Bear Valley suite. The Poso Flat unit mesoscopically resembles the Tonalite of Bear Valley Springs, although its K-feldspar modes place it marginally within the granodiorite field. The Poso Flat unit is considered the northern, relatively shallow-level terminus of the Bear Valley suite, although there are small screens of the Bear Valley Springs unit north of the Poso Flat unit between Needles and Kern River suite rocks. Rocks of the Needles suite in general cut and bound the northern limits of the Bear Valley suite (Fig. 2).

New U/Pb zircon age data on the Bear Valley suite are presented here for a commingled mafic intrusive body within the Bear Valley Springs unit (B1), four samples of the Bear Valley Springs (B2-B5), the type location of the Mount Adelaide unit at Mount Adelaide (B8), and two samples from the Poso Flat unit (B9 and B10). Also, two 100 m-scale enclaves of Early Cretaceous tonalite, not readily distinguished in the field from much of the Bear Valley unit, were dated here (B6 and B7). Early Cretaceous tonalite and tonalite gneiss enclaves are common within the deeper-level exposures of the Bear Valley Springs unit, and may be more common than what is readily recognized.

Sample B1 is from a 2 km x 4 km diorite enclave that is partly commingled with and lying concordantly within foliated Bear Valley Springs tonalite. Such mafic members of the suite range up to ~5 km in diameter, and down to meter-scale disrupted

dike and inclusion swarms. Some of the larger bodies range in composition from hornblende diorite to hornblende (±pyroxenes and rare olivine) gabbros and metagabbros. Sample B1 yielded one sparse fine fraction with an internally concordant age of 101.8±0.4 Ma. The proximal Bear Valley Springs host for the diorite is typical of much of the tonalite, being steeply foliated and rich in deformed mafic inclusions. Within ~3 km of the diorite enclave, however, lies a nonfoliated, inclusion-poor zone of the tonalite that cuts foliated inclusion-rich tonalite. Sample B2, from this more homogeneous zone, yields an externally concordant age of 101.0±0.3 Ma (Fig. 7). The sample B1 and B2 data, along with the intrusive field relations, bracket the age of the foliated inclusion-rich tonalite to ca. 101.5 Ma as well.

Samples B3 and B4 are from the Bear Valley Springs unit in the Walker Basin area (Fig. 2). These samples are from foliated, mafic inclusion-rich tonalite typical of the Bear Valley Springs unit. Sample B3 yields a U/Pb age spectrum indicating a 100.1±0.7 Ma age. The age spectrum includes discordant grains indicative of minor inheritance. Sample B4 yields a fine internally concordant fraction and coarser slightly discordant fractions that disperse off of concordia progressively with grain size (Fig. 7). Such dispersion is suggestive of very minor inheritance of older (Proterozoic?) grains, but to such a limited extent that a concordia intercept solution carries little meaning. The internally concordant age of 101.5±0.4 Ma is interpreted as an approximate igneous age. Small screens of the Bear Valley Springs tonalite that are locally rich in commingled gabbros lie between Needles suite plutons and older pendant and Kern River suite rocks at ~35.75°N. Sample B5 is from the western screen. It yields a U/Pb age spectrum suggesting an igneous age of 102.6±3.9 Ma. These small screens constitute the only

known locations where the tonalite is in contact with older Kern River suite rocks. The eastern screen possesses local sill-like structures, along with commingled gabbros, suggesting that it was stacked in beneath pendant and Kern River suite rocks. Such structural relations are consistent with the shallow emplacement levels of the Kern River suite, whose terminal emplacement ages merge with the ca. 102 Ma onset of Bear Valley Springs tonalite emplacement in the region.

Structural and textural relations and age data resolve two significant screens of Early Cretaceous tonalite within the Tonalite of Bear Valley Springs. In the Walker Basin area an ~500 m wide screen of foliated biotite tonalite occurs along the Bear Valley Springs northern contact with pendant rocks (Fig. 3). Sample B6 is from this screen. It yields a U/Pb age spectrum indicating an age of 108.9±1.3 Ma (Fig. 6). The age spectrum includes discordant grains indicative of minor to modest inheritance of older zircon. An additional enclave of Early Cretaceous tonalite was discovered ~6 km west of the sample B6 enclave, across the KCF (Fig. 2). This enclave is a minimum of 500 m across, although poor exposure limits its detailed map extent. Sample B7 is from this enclave. It yields a U/Pb age spectrum indicating an age of 113±1.0 Ma. The scatter of the data points of this spectrum permit the possibility of both minor inheritance in some grains and minor disturbance in other grains, presumably during engulfment by the Bear Valley Springs tonalite.

The Mount Adelaide and Poso Flat units of the Bear Valley suite are much more homogeneous than the Bear Valley Springs unit, and typically lack the synplutonic deformation fabric of the latter. Sample B8 is from the Mount Adelaide unit at its type location near the western edge of the Sierra (Fig. 2). It yields an externally concordant

age of 98.6±0.6 Ma (Fig. 7). A duplicate split of this sample yields a U/Pb age spectrum indicating an age of 98.2±0.4 Ma, thus, an age of 98.4±0.3 Ma is assigned for this sample. This age matches the youngest age determined for the Bear Valley suite, which was determined for the Bear Valley Springs unit within the deep-level exposures south of the study area (Saleeby et al., 1987). The Mount Adelaide unit of the sample B8 area is observed crosscutting the adjacent Bear Valley Springs unit as well as its synplutonic deformation fabric, consistent with the age data.

Samples B9 and B10 are from the Poso Flat unit. Sample B9 yields an externally concordant age of 101.1±0.3 Ma (Fig. 7). Sample B10 yields a U/Pb age spectrum indicating an age of 100.2±0.5 Ma (Fig. 6). The Poso Flat unit, like the Bear Valley Springs unit, contains recognizable internal contacts that suggest the age difference between samples B9 and B10 could be real, and of geological significance.

In summary, the zircon age data presented here for the relatively shallow-level exposures of the Bear Valley intrusive suite in the study area indicate a clustering of igneous ages for the Tonalite of Bear Valley Springs, including commingled mafic intrusives and the Mount Adelaide and Poso Flat units of ca. 98-102 Ma. This is similar to the age range that was determined for much of the suite in the Tehachapi complex to the south, and together these data sets indicate that most of the Bear Valley suite was assembled over the same time interval along its entire ~100 km north-south extent. The Bear Valley Springs unit is characterized by myriad compositionally similar small intrusions, typically displaying steeply-dipping synplutonic deformation fabrics accentuated by the remnants of deformed commingled mafic dikes. The various members of the Bear Valley Springs unit also display a wide range of Sr_i (0.70424-

0.70601), as high as 0.70677 adjacent to migmatitic metasedimentary enclaves (Saleeby et al., 1987; Kistler and Ross, 1990; Pickett and Saleeby, 1994). In contrast, the Mount Adelaide and Poso Flat units are more homogeneous at outcrop and map scale, possess a much more restricted range of Sr_i (0.70427-0.70503), and appear to have been emplaced over the more restricted time interval of ca. 100-98 Ma. Furthermore, the Mount Adelaide and Poso Flat units are restricted to exposure levels of ≤4 kb, whereas the Bear Valley Springs unit extends from ~8 kb to perhaps as shallow as ~2 kb levels in the north where it intrudes rocks of the Kern River suite (Ague and Brimhall, 1988; Pickett and Saleeby, 1993; Nadin, Chapter 3).

Intrusive Suite of the Needles

The northern exposures of the Bear Valley intrusive suite are cut by the southern end of a belt of mainly granodioritic to locally tonolitic plutons referred to here as the Needles suite, named after a prominent glaciated summit that lies at the northern margin of the study area, and which is underlain by the Granodiorite of the Needles (Fig. 2). Some of the Needles suite plutonic rocks resemble in mesoscopic structure and texture some phases of the Bear Valley Springs unit as well as the more uniform Mount Adelaide and Poso Flat units (Ross, 1989). The Needles suite plutons occur as smaller, commonly nested, bodies as compared to the principal units of the Bear Valley suite. This distinctive belt of plutons continues northwestwards beyond the limits of the study area (du Bray and Dellinger, 1981). The Needles suite plutons also contrasted with the Bear Valley suite by their higher and more restricted range of Sr_i (0.70616-0.70669, with outliers as high as 0.70742), and an overall younger age range of emplacement (ca. 96-

100 Ma).

Principal plutons of the Needles suite for which new zircon age data are presented include: the Granodiorite of Alder Creek, the Granodiorite of Brush Creek, the Tonalite of Dunlap Meadow, the Granodiorite of Pine Flat, the Granodiorite of Alta Sierra, the Granodiorite of Peppermint Meadow, the Granodiorite of the Needles, and the Granodiorite of Wagy Flat (Fig. 2 and Table 1). The Alder Creek unit is the oldest dated pluton of the suite. Textural and structural variations in this unit indicate that it is a composite body. Sample N1 is from the most homogeneous and aerially extensive zone of the pluton. It yields a U/Pb age spectrum indicating an age of 100.9±1.0 Ma (Fig. 6). The spread of data for the N2 spectrum presents the possibility that the Alder Creek body is younger (ca. 98-100 Ma) than the mean age given. The granodiorite of Brush Creek is a distinct member of the Needles suite in that it is notably melanocratic, enriched in mafic enclaves, and is relatively old compared to most other plutons of the suite. The Brush Creek body is nested in along the marginal zone of the much larger Peppermint Meadows pluton, against the Fairview pendant (Fig. 2). Sample N2 from the Brush Creek body yields an externally concordant age of 100.6±0.4 Ma (Fig. 7). This age, along with the caveat given above for the age data on the Alder Creek pluton, leads to a preferred upper age bound for the Needles suite of ca. 100 Ma.

Samples N3 and N4 are from the Tonalite of Dunlap Meadow and the Granodiorite of Pine Flat, respectively. Map relations of these two bodies suggest that they are part of a concentrically zoned pluton, with the more felsic phases in the interior (Fig. 2). Sample N3 yields an externally concordant age of 98.5±0.5 Ma, and sample N4 an externally concordant age of 98.3±0.4 Ma (Fig. 7).

The northernmost plutons studied here from the Needles suite consist of the granodioritic plutons of Peppermint Meadows and the Needles. Textural variations and local internal contacts within and between these bodies suggest that they are each composites of several compositionally and texturally similar intrusive sequences. Samples N6 from the Peppermint Meadows pluton and N7 from the Needles pluton yield similar U/Pb age spectra that are characteristically noisy. The N6 spectrum suggests an age of 97.4±1.5 Ma, and the N7 spectrum an age of 96.7±0.9 Ma (Fig. 6). Sample N7 is on the margin of the PKCF, and exhibits a modest ductile deformation fabric (Nadin, Chapter 4). Part of its age scatter could be due to minor disturbance of its more labile grains. Sample N8 is from the interior of the Needles pluton. It is from ~5 km west of the PKCF, and it has a pristine igneous texture. It yields an array of internally concordant to slightly discordant fractions, suggesting an age of 96.0±0.5 Ma (Fig. 7). The convergence of the N6, N7 and N8 ages strongly suggests that the Peppermint Meadows-Needles composite of texturally and compositionally similar plutons is ca. 96 Ma.

The southeastern end of the Needles suite consists of the texturally and structurally distinct granodiorites of Alta Sierra and Wagy Flat. These are relatively uniform northwest-striking elongate plutons that are both offset ~8 km dextrally by the KCF (Fig. 2). They cut the northeastern end of the Bear Valley suite, and along with the Alder Creek body they have calved off a screen(s) of marginal phase gabbros and tonalities of the Bear Valley suite and their host pendant rocks. Sample N5 is from the Alta Sierra pluton and yields a meager zircon population with a U/Pb age spectrum suggesting an igneous age of 98.3±3.6 Ma (Fig. 6). Samples N9 and N10 are from the Wagy Flat pluton, on opposite sides of the KCF (Fig. 2). Sample N9 to the west of the

KCF yields a U/Pb age spectrum suggesting an igneous age of 95.5±1.2 Ma (Fig. 6). The discordant data points are clearly the products of inheritance. The clustering of this component's U/Pb ages at ca. 115 Ma suggests incorporation of batholithic zircon from an Early Cretaceous source, akin to the widespread screens that are dispersed within the Bear Valley suite (cf. samples B6 and B7). Sample N10 to the east of the KCF yields a U/Pb age spectrum suggesting an age of 95.9±2.1 Ma (Fig. 6). The Granodiorite of Wagy flat appears to be the youngest member of the Needles suite, although it could be the same age as the Peppermint Meadows-Needles complex.

The apparent age range of the Needles intrusive suite is ca. 95.5-100.9 Ma. The Needles suite age range is clearly offset from the ca. 98-102 Ma range of the Bear Valley suite. Clear contrasts between these two suites are also exhibited by the more uniform and overall more felsic composition of the Needles suite, and by its consistently higher Sr_i values (Table 1). The Needles suite Sr_i values are not only notably more radiogenic, but its overall systematics is more orderly. Multiple samples from individual units form strong linear arrays on Rb/Sr evolution diagrams, and a number of units share the same arrays (Kistler and Ross, 1990). Isochron ages derived from these arrays agree, within uncertainty, with the zircon ages as well. In contrast, a large sample set from the various intrusive units of the Bear Valley suite shows little or no systematics and a wide range of Sr_i (Saleeby et al., 1987; Pickett and Saleeby, 1994; Kistler and Ross, 1990). These relations suggest a greater degree of homogenization in the source region for the Needles suite magmas, and little or no contamination upon ascent.

Intrusive Suite of the South Fork

The South Fork intrusive suite is named for a relatively small cluster of ca. 94-100 Ma plutons spanning leucogranite, mafic granodiorite, diorite and gabbro that are incised by the South Fork Valley of the Kern River (Fig 2). This suite is unique by the degree of deformation and metamorphism that its wallrock pendants experienced during its intrusion. This included the development of pervasive high-strain metamorphic tectonites in the Isabella pendant, and extensive migmatization of psammite-pelite units along relatively broad contact aureoles (Saleeby and Busby-Spera, 1986; Saleeby and Zeng, 2006). This suite is also distinguished by its wide range of Sr_i (0.70593-0.73500), as well as the presence of marginal zones in some plutons that exhibit extensive zircon entrainment by the intermixing of melt products from adjacent migmatitic pendant rocks (these complexities are discussed in Kistler and Ross, 1990; Zeng et al., 2005, 2006; Saleeby and Zeng, 2006). We present here new U/Pb zircon age data on the three most aerially extensive plutons of the South Fork suite, which consist of the Quartz Diorite of Cyrus Flat, the Alaskite of Sherman Pass, and the Granodiorite of Rabbit Island (Fig. 2).

The Quartz Diorite of Cyrus Flat consists of a hornblende-rich gabbroic zone concentrated along its current west-central map area. This mafic zone is mantled to the north, east and south by intergradational rocks ranging from quartz diorite to mafic granodiorite. The western margin of the pluton is ductiley sheared by the PKCF (Nadin, Chapters 4 and 5), and intruded by the Granite of Cannell Creek of the Domelands suite. The eastern margin of the Cyrus Flat pluton is interleaved with the Granodiorite of Rabbit Island as well as a series of leucogranite dikes (Plate 1). Prior to truncation by the PKCF and intrusion of the Cannell Creek pluton, the Cyrus Flat body may have formed a

concentrically zoned pluton, or ring dike complex, akin to a number of other relatively small mafic plutons that have been studied in detail in the southern SNB (Mack et al., 1979; Clemens-Knott and Saleeby, 1999). We present new U/Pb zircon data for a hornblende-hypersthene leucogabbro form the western core zone of the Cyrus Flat pluton (sample S1). Its meager fine zircons yield an internally concordant age of 99.6± 0.3 Ma (Fig. 8). Data for highly contaminated zircon populations from its marginal zones are presented in the context of migmatitic wallrock interactions in Saleeby and Zeng (2006).

The principal felsic units of the South Fork suite are dispersed along a NW-trending belt, partly within the eastern margin of the PKCF, but to a greater extent encased as a series of enclaves within Domeland suite granitoids (Fig. 2). These consist of the Alaskite of Sherman Pass and the Granodiorite of Rabbit Island (Fig. 2). Sample S2 is from the elongate alaskite pluton, near its northern terminus. This sample yields a U/Pb age spectrum suggesting an igneous age of 99.3±0.7 Ma (Fig. 9). Alaskitic (leucogranite) dikes are locally commingled with the Cyrus Flat mafic pluton, and the correspondence of the S1 and S2 ages, within uncertainty, further suggests that the Sherman Pass and Cyrus Flat plutons were at least in part comagmatic. The Granodiorite of Rabbit Island is a composite body consisting of mafic granodiorites, and microdioritic coherent and commingled dikes and inclusion swarms. The mafic granodiorites were emplaced over an apparent 5 m.y. time interval, as were a smaller series of South Fork suite granodioritic plutons, which are intimately involved in wallrock migmatization along the southwest margin of the Isabella pendant (Saleeby and Zeng, 2006). Sample S3 is from the most homogeneous phase of the Rabbit Island pluton, which is transected by the South Fork Valley arm of Lake Isabella. It yields an externally concordant zircon age

of 99.0±0.4 Ma (Fig. 8). This relatively homogeneous phase of the pluton extends southeastward across the South Fork Valley as a lobe-like feature within Domelands suite granitoids. Much of this lobe appears to be more heterogeneous than the pluton to the north is, although internal structural relations are obscured by crosscutting Domelands dikes. Sample S4 is from a relatively homogeneous zone of Rabbit Island granodiorite of this area (Fig. 2). It yields a marginally externally concordant age of 97.8± 0.7 Ma (Fig. 8). The slight displacement of the second coarser fraction off of concordant suggests minor inheritance, leading to the weighting of the finer internally concordant fraction's U/Pb age as the interpreted igneous age.

The northern tip of the contiguous Rabbit Island pluton is attenuated along the eastern margin of the PKCF. Sample S5 is from a ductiley deformed mafic granodiorite of this zone. It yields an externally concordant age of 97.0± 0.4 Ma (Fig. 8). Younger phases of the Rabbit Island composite body are petrographically similar to the principal older phases discussed above, although they typically are poorer in commingled mafic dikes and inclusion swarms. Sample S6 is from such a younger phase, at the southern end of the pluton. It yields a U/Pb age spectrum suggesting an igneous age of 94.9±0.8 Ma (Fig. 9). Sample S7 is from a younger phase of the pluton to the north, where it begins to become deformed in the PKCF. This sample yields a U/Pb age spectrum suggesting an igneous age of 93.7±1.1 Ma.

The zircon age data presented here suggest that the South Fork intrusive suite was emplaced over the ca. 94-99 Ma time interval. It was emplaced under deeper-level and higher-strain conditions than the roughly coeval Needles suite to the west (Nadin, Chapter 3; Saleeby and Zeng, 2006). As discussed below, Domelands suite intrusive

activity began at least locally as South Fork intrusive activity ceased. The South Fork suite plutons were disrupted and deformed both by the PKCF to the west, and by the incremental emplacement of the younger Domelands suite to the east.

Intrusive Suite of the Domelands

The Domelands suite is the most extensive intrusive suite of the study area. It is restricted to the area east of the PKCF, and constitutes one of the principal protolith elements within the principal damage zone of the PKCF (Nadin, Chapters 4 and 5). This suite consists of three regionally extensive plutonic units, including the Granodiorite of Claraville, the Granite of Castle Rock, and the Castle Rock granitic dike swarm(s) (Fig. 2). The Claraville unit is also referred to as the Whiterock (nonporphyritic) facies of the Granite of Castle Rock (Ross, 1994). We retain the term Claraville, which was originally defined south of the study area where it has yielded U/Pb zircon dates within the 91±1Ma time interval (Saleeby et al., 1987; Wood and Saleeby, 2006). The Castle Rock unit is distinguished in this study by its pink K-feldspar megacrystic texture, and common aplitic to pegmatitic granitic dikes. The Claraville locally contains pink K-feldspar phenocrysts that resemble those of the finer phenocrystic Castle Rock. The Castle Rock unit appears to be 1-3 m.y. younger than the Claraville unit. The Castle Rock granitic dike swarms consist of myriad small tabular intrusions, isolated and composite dikes, and inter-dike bridges. Within the PKCF damage zone, the Castle Rock unit also contains variably transposed dikes and concordant sheets. The Granite of Onyx, also grouped into the Domelands suite, appears to be principally dike rock as well, but it is distinctly older than the Castle Rock dikes. The Castle Rock granitic dike unit that is differentiated on

Figure 2 is arbitrarily defined as the region where clearly resolvable felsic dikes constitute greater than 50 percent of the outcrop area. The Castle Rock dike unit contains screens of both Claraville and Castle Rock granitoids. Internal contact relations, textural variations, and the U/Pb age data indicate that much of the Castle Rock unit was constructed from numerous dikes and/or small tabular plutons. The Claraville unit possesses internal contacts as well, but its internal units appear to underlie map areas larger than those of the Castle rock unit.

The large-volume units of the Domelands suite were emplaced between ca. 87-92 Ma. Some of the smaller units were emplaced between ca. 93-95 Ma, thus overlapping with the youngest units of the South Fork suite. Domelands granitoids contrast sharply with the more mafic units of the South Fork suite, and are distinguished from the South Fork leucogranites by higher K-feldspar and biotite contents. Domelands suite rocks also show a much more restricted range of Sr_i (0.70704-0.70930) than the 0.7093-0.7350 range exhibited by the South Fork suite (Kistler and Ross, 1990; Zeng et al., 2006).

The oldest units of the Domelands suite are the Granite of Long Meadow, the Granite of Cannell Creek, and the Granite of Onyx. These plutons lie in contrasting structural positions. The Long Meadow body is a large enclave within Castle Rock megacrystic granite. Sample D1 from the Long Meadow granite yields a U/Pb age spectrum suggesting an igneous age of 95.2± 0.8 Ma (Fig. 9). The Granite of Cannell Creek is a high-strain blastomylonite the lies concordantly within the PKCF (Plate 1). It runs for a strike distance of ~12 km within the shear zone, where to the north it interfingers with and is replaced by veri-textured mylonitic Castle Rock granite, mainly dikes, informally named Goldledge Granite by Busby-Spera and Saleeby (1990) (Plate

1). Both the Cannell Creek and "Goldledge" granites bear critical structural and age relations constraining the deformation history of the PKCF (Nadin, Chapter 5). These are discussed further below in the context of other Domelands suite age relations. Sample D2 is from the Cannell Creek unit. Three natural size fractions yielded two externally concordant ages of 94.6±0.4 Ma, and an externally discordant/ internally concordant age of 93.4±0.4 Ma on its fine fraction. One of the coarser fractions was abraded to a well-rounded state to test if it had undergone grain margin disturbance during high-temperature mylonitization. It yielded an internally concordant age of 94.8±0.4 Ma, which agrees with the two coarser fractions (Fig. 8). These data are interpreted to mark a 94.7±0.4 Ma igneous age with the finer fraction having undergone minor disturbance during high-temperature strain and annealing. The Granite of Onyx consists primarily of fine-grained granitic dike rock. Sample D3 from the Onyx dikes yields a U/Pb age spectrum suggesting an igneous age of 93.0±1.5 Ma (Fig. 9). As discussed below, this is distinctly older than the widespread Castle Rock dikes. The only clearly resolvable host for the Onyx granite is the Rabbit Island granodiorite of the South Fork suite. The map relations of the South Fork and Domelands suites (Fig. 2) suggest that the Domelands suite grew from a core of Onyx and Long Meadow dikes and tabular plutons that initially intruded and dispersed South Fork suite host rocks.

The Claraville and Castle Rock granites are larger-volume units of the Domelands suite. Based on our age data and the textural criteria presented above, we extend the Claraville unit much further north than Ross (1995) did. Samples D4, D5, D6 and D7 are representative of large areas of the Claraville unit. D4 yields a U/Pb age spectrum suggesting an igneous age of 92.5± 0.7 Ma (Fig. 9). There is no reason to suspect that the

Claraville of this region suffered any subsolidus disturbances. Sample D5 yields a discordant array of data points with a 91.9± 0.4 Ma lower intercept and a 1669+140/-120 Ma upper intercept (Fig. 5). This array is interpreted as a trajectory marked by inheritance, with the lower intercept approximating the igneous age and the upper intercept an averaged age of the inherited component. Sample D6 yields a U/Pb age spectrum suggesting an igneous age of 91.2± 1.9 Ma (Fig. 9). The grouping of a significant number of the aberrant points at ca. 111 Ma and ca. 170 Ma strongly suggests the incorporation of older batholithic zircon. The two older ages of ca. 215 Ma and ca. 260 Ma could represent highly disturbed Proterozoic detrital grains from metaclastic pendant rocks or non- to little disturbed batholithic zircon. Permo-Triassic as well as Jurassic batholithic units lie adjacent to the Claraville unit east of the Kern Plateau shear zone (Dunne and Saleeby, 2006). The aberrant ages of the D6 spectrum are therefore suggested to be a source inheritance feature. Sample D7 yields a U/Pb age spectrum suggesting an igneous age of 90.0± 1.9 Ma.

Zircon age data presented above suggest that the Claraville unit was emplaced between ca. 92.5 and 90 Ma, a slightly wider range of ages than those determined for the unit to the south of the study area (Saleeby et al., 1987; Wood and Saleeby, 2006). This age range suggests that Claraville magmatism ceased as the megacrystic Castle Rock series of intrusions began their emplacement.

Samples D9, D10 and D11 are from relatively homogeneous Castle Rock granite. Sample D9 was analyzed by both techniques as another calibration point. It yields a U/Pb age spectrum suggesting an igneous age of 89.5± 0.5 Ma (Fig. 9). By the TIMS-ID technique it yields externally concordant fractions with an age of 89.2± 0.1 Ma (Fig. 8).

The igneous age for sample D9 is taken as 89.3± 0.2 Ma. Sample D10 yields externally concordant ages suggesting an igneous age of 89.0± 0.5 Ma (Fig. 8). Sample D11 lies proximal to the PKCF (Fig. 2). It yields an externally concordant age of 87.1± 0.4 Ma. The western edge of the D11 mass is progressively deformed and intruded by granitic dikes progressing westward into the PKCF.

The terminal phase of Domelands suite magmatism was dominated by the emplacement of widespread felsic dikes along with small tabular megacrystic granite bodies. This phase of Domelands magmatism is most pronounced north of latitude 35.75° N, and is virtually absent in the southern reaches of the study area and continuing southward to the terminus of the SNB. Such magmatism is shown to have lasted locally to ca. 83±1 Ma (Busby-Spera and Saleeby, 1990). We focus on two aspects of the terminal magmatism: 1) Structural and age relations of PKCF deformation; and 2) Construction of the Castle Rock felsic dike unit.

Structural and age relations along the PKCF indicate that cessation of high-magnitude ductile strain was time transgressive and took place during emplacement of the Domelands suite (Nadin, Chapter 3). Batholithic rocks that lie within the principal damage zone consist of Castle Rock dikes and small tabular megacrystic bodies north of ~35.75° N, the Cannell Creek granite and rocks of the Kern River and South Fork suites between latitudes ~35.75° and 35.5° N, and the Claraville, Bear Valley, and southernmost Needles suite rocks to the south (Fig. 2; Plate 1). Sample D12 is from a mildly pegmatitic leucogranite dike from the southern segment of the damage zone. It crosscuts at a high angle the mylonitic fabric in the margin of the Claraville granodiorite, which is the local expression of the eastern domain of the PKCF. It yields two externally

concordant fractions, suggesting an igneous age of 86.1±0.4 Ma (Fig. 8). These data, in conjunction with field relations, bracket the main phase of ductile deformation along the southern segment of the PKCF in the study area to between ca. 92 and 86 Ma. Sample D13 is from a mylonitic pegmatitic granite dike that partially crosscuts and is partially transposed into the high-strain blastomylonitic fabric of the Cannell Creek granite. This sample, therefore, records part of the ductile deformation history of the PKCF. Three natural-size fractions and one abraded split of the intermediate size fraction yield externally concordant ages suggesting an igneous age of 85.7±0.5 Ma (Fig. 8). These data, in conjunction with field relations, bracket a significant component of the main-phase ductile deformation along the central segment of the PKCF in the study area to between ca. 94-85 Ma. As discussed further below, structural and age relations within the "Goldledge" granite indicate continued high-strain ductile deformation in intrusives of ca. 85±1 Ma age, and a substantial waning of ductile deformation at the time of the apparent ca. 83±1 Ma termination of Domelands magmatism.

One sample (D14) was taken from the Castle Rock felsic dike unit shown on Figure 2. Dikes of this unit, as well as many dikes that are dispersed within the Claraville and Castle Rock units removed from the PKCF, rarely have significant ductile deformation fabrics. Sample D14 has a U/Pb age spectrum suggesting an igneous age of 84.2± 1.5 Ma (Fig. 9). The three grains that yield ages of ca. 173 Ma resemble the principal inherited component observed in the nearby D6 Claraville sample. These, as well as the aberrant grain yielding an age of ca. 420 Ma, are interpreted below as source inheritance contaminants. The D14 age data coupled with D12, D13, and "Goldledge" data suggest that felsic dike emplacement was widespread throughout the northern half of

the Domelands suite between ca. 86 and 83 Ma. Domelands suite magmatism was most prolific between ca. 93 and 87 Ma, and locally began as early as ca. 95 Ma. These age relations as well as structural and textural relations indicate that the Domelands suite was assembled over an approximate 10 m.y. time interval with local dike emplacement continuing for an additional ~2 m.y.

Discussion

In the context of this thesis, this section of the paper has been abbreviated from a larger version that integrates the geochronological data presented above with that of the Tehachapi complex (Saleeby et al., 1987, 2006; Pickett and Saleeby, 1994, Wood and Saleeby, 2006) to provide a temporal framework that links the shallow batholithic and supra-batholithic volcanic levels of the study area to the lower crustal complex. In the lengthier version, the physical and temporal continuity along the oblique crustal section provides a basis to consider several important issues in SNB petrogenesis and tectonics, including: 1) composite batholith crustal structure, 2) magma production rates in Cordilleran-type arcs, 3) pluton emplacement mechanisms, 4) batholith compositional variations as fingerprints of source versus ascent and emplacement processes, and 5) kinematic relations of intra-arc deformation. In this abbreviated discussion, we visit only topic #5.

Chronology of Regional Deformation

U/Pb zircon age data presented here, in conjunction with other geochronological and structural studies, help constrain the timing and kinematic relations of regional

deformation that affected the southern SNB. In terms of relative chronology, the principal structures of the study area include: 1) pre-batholithic ductile deformation including folding, thrusting and cleavage development of the Kings sequence pendant rocks, 2) at least local brittle high-angle faulting and uplift of the Kings sequence, and unconformable overlap by the Erskine Canyon sequence, 3) high-magnitude ductile strain and local migmatization of pendant rocks in conjunction with the intrusion of the South Fork intrusive suite, 4) east-side-up ductile thrusting along the PKCF, 5) dextral-sense ductile shear and displacement along the PKCF as well as the Kern Canyon fault, and 6) brittle deformation along the Kern Canyon and related faults. The age data that we have presented above places relatively tight absolute constraints on 2 through 5 above, and only bounding constraints on 1 and 6. Below we focus on 4 and 5.

The evolution of the PKCF is an essential factor in the tectonics of the southern SNB. The PKCF is distinguished from the KCF by a wide zone of ductile deformation (~1-2 km) in contrast with more focused brittle deformation, and by a southward bifurcation of the two structures at latitude ~35.5° N (Fig. 2; Nadin, Chapter 6). Dextral separation along the Kern Canyon fault of between ~8-16 km has been described by Moore and DuBray (1978) and Ross (1986). How these offsets shunt into the PKCF is a subject too complex to discuss here in detail, as are details of the offset history of the PKCF (see Nadin, Chapters 4 and 5). The total offset history of the PKCF is highly obscured due to the fact that a significant component of its history may pre-date the emplacement of its east-bounding ca. 90-85 Ma large-volume plutons. Vertical components of slip, which have affected these as well as older plutons, have imparted significant along-strike variations in the depth of exposure gradients of the oblique crustal

section along opposing walls of the PKCF (Ague and Brinhall, 1988; Pickett and Saleeby, 1993; Nadin, Chapter 3). This pattern and the fact that the regional trace of the Sr_i=0.706 isopleth of the SNB coincides with the southern ~75 km of the PKCF (Kistler and Ross, 1990; Pickett and Saleeby, 1994) suggests that it is a much more fundamental structure than that implied by the ~8-16 km of dextral separation referenced above.

Broad constraints on the displacement history of the PKCF were posed by Busby-Spera and Saleeby (1990). Direct evidence for the initiation of large-magnitude ductile strain along the PKCF is recorded in the structural and textural relations of the South Fork intrusive suite, and the Granite of Cannell Creek (Nadin, Chapters 3 and 5; Saleeby and Zeng, 2006). These studies show continuity in time and space between the high-magnitude ductile strain and migmatization in the pendant rocks that host the South Fork suite (ca. 95-100 Ma), progressing westward to synmagmatic mylonitization of the Cannell Creek granite (ca. 94.7 Ma). This phase of east-side-up ductile thrusting resulted in a ~2-5 kb discontinuity in depth of exposure across the PKCF in the Lake Isabella region (Nadin, Chapter 3). High-temperature dextral-sense shear bands are superimposed on the steeply-dipping reverse-sense ductile fabrics of the Cannell Creek granite as well as on its high-grade wallrocks. The blastomylonitic fabrics of both phases of deformation in the Cannell Creek and the fabrics of its hosting pendant rocks arose in amphibolite facies conditions, reflecting deformation under synplutonic to hot subsolidus conditions. Ar/Ar age data from the Cannell Creek granite and from its high-strain pendant rocks indicate cooling and closure through Ar blocking temperature in hornblende (500˚ C) at ca. 90 Ma (Dixon; 1995; Wong, 2005). These relations indicate that east-side-up ductile thrusting along the PKCF had started at least by ca. 95 Ma, and that dextral shear had

commenced between ca. 90-94 Ma.

Oblique dextral shear under high-grade ductile conditions is also recorded along the west margins of the ca. 89.3-92.5 Ma Claraville granodiorite, and the ca. 85.0-89.3 Ma Castle Rock granite (Busby-Spera and Saleeby, 1990; Nadin, Chapter 5). The thrust component of displacement increases substantially southward from latitude ~35.5°N, principally along the margin of the Claraville body (Nadin, Chapter 3; Wood and Saleeby, 2006). Structural and age relations of dextral shear in the Castle Rock body presented in Busby-Spera and Saleeby (1990) are refined here. This work noted that a ca. 83±1Ma non-deformed phase of the Castle Rock granite crosscuts a pervasively mylonitic 85±1Ma phase. Subsequent field investigations have revealed local high-temperature dextral shear bands within the ca. 83 Ma phase, suggesting that this phase of the Castle Rock granite records the waning, as opposed to cessation, of ductile dextral shear. Superimposed brittle fabrics of this area are only poorly constrained in age to have post-dated the ductile deformation.

Time constraints on the waning of ductile deformation along the PKCF posed along the western edge of the Claraville granodiorite differ from those of the Castle Rock granite. The western margin of the Claraville granodiorite was pervasively sheared at high temperatures along the southern segment of the PKCF. Kinematic indicators along this high strain zone indicate components of both dextral and east-side-up thrust displacement (Nadin, Chapters 3, 4, and 5). Structural relations of the sample D12 leucogranite dike, discussed earlier, indicate that the bulk of the ductile strain of this area occurred prior to ca. 86±0.4 Ma. The ~3 m.y. difference in the duration of the ductile deformation history implied for the southern versus northern segments of the PKCF may

record the inception of the KCF, and its shunting into the northern PKCF. The overall age and structural relations also suggest that early ductile deformation along the PKCF was dominated by east-side-up thrust displacements, and progressively more dextral displacements were imparted with time.

The temporal relations of ductile thrusting and dextral shear along the PKCF may be correlated to the timing and kinematic patterns of regional deformation of the Tehachapi complex to the south of the study area, and the central SNB to the north. In the Tehachapi complex, crustal thickening related to the onset of intra-arc thrusting commenced between ca. 90-100 Ma, and vigorous uplift and unroofing of the deep-level batholithic rocks was operative between ca. 90-94 Ma (Saleeby et al., 2006). This study, in conjunction with that of Grove et al. (2001), also shows that the subduction accretion assemblages of the Rand schist were displaced eastward by regional low-angle subduction from the Franciscan trench to beneath the Tehachapi complex between ca. 86-93 Ma. The timing of such lithosphere-scale thrusting and compressional deformation matches well with ca. 95 Ma onset of ductile thrusting along the PKCF and its ca. 86 Ma termination along its southern segment. In the central SNB, steeply dipping west-directed reverse-sense ductile shear zones were active between ca. 95-100 Ma, and dextral-sense ductile shear zones were active between ca. 78-88 Ma (Tobisch et al., 1995). These also match the thrust-dominated and dextral-dominated deformation phases of the PKCF, although ductile shear along the PKCF was waning by ca. 83 Ma. Rapid unroofing of the southernmost SNB in the ca. 95-85 Ma time interval may account for imbrittlement of the post-83 Ma dextral shear, while slower unroofing to the north may account for a more protracted interval of ductile deformation.

Finally, the intense history of intra-arc deformation and unroofing that is recorded for the southern SNB is also recorded in the depositional history of the Great Valley forearc basin, as well as some metaclastic rocks of the Franciscan complex. Petrographic and stratigraphic studies of the Great Valley forearc sequence reveal an acceleration of SNB unroofing commencing in strata that are roughly constrained to be ca. 90 Ma in age (Mansfield, 1979). Furthermore, the entire late Mesozoic forearc basin sequence was eroded off the southernmost Great Valley between Late Cretaceous and Paleocene time (Reid and Cox, 1989), presumably in parallel with crustal-scale tilting and exhumation of the southernmost SNB oblique crustal section. Rapid unroofing of the southern SNB and the adjacent southern California batholith is also recorded by U/Pb ages of detrital zircon from Upper Cretaceous strata of the southern Franciscan complex, and the Rand and related schists that tectonically underlie the Tehachapi complex and southern California batholith (Barth et al., 2001; Grove et al., 2001; Jacobson et al., 2004). The timing of such sedimentation coincides with early PKCF ductile thrusting, suggesting the fault played a role in exhumation of the southernmost part of the SNB (Nadin, Chapter 3). Thus a regionally coherent story is emerging concerning the timing and kinematics of Late Cretaceous intra-arc deformation and related unroofing of the central to southernmost SNB.

Summary and conclusions

We present an extensive U/Pb zircon age data set for the southern Sierra Nevada batholith (SNB). These data tie together earlier published regionally extensive U/Pb zircon age data sets from the central SNB to the north and the deep-level batholithic

rocks of the Tehachapi complex to the south. These data, in conjunction with regional field mapping, establish physical continuity and temporal continuity in pluton emplacement along an oblique crustal section traversing volcanic and shallow-level plutonic levels in the north to lower crustal batholithic (~35km) levels in the south. The establishment of such continuity, along with the details of the age relations, provides a framework for further analysis of a series of issues in batholith primary structure, pluton emplacement mechanisms, factors influencing the compositional evolution of batholithic magmas, and regional deformations superimposed on the southern SNB.

Based on the U/Pb zircon age data, our own mapping, and the mapping and derivative petrographic/geochemical data of published studies (Saleeby et al., 1987, 2006; Ross, 1989, 1995; Kistler and Ross, 1990), we define five intrusive suites in the southern SNB between latitudes 35°N and 36.2°N. These consist of: 1) the granitic Kern River suite (ca.102-106 Ma), 2) the tonalitic to gabbroic Bear Valley suite (ca.102-98 Ma), 3) the gabbroic to granodioritic South Fork suite (ca. 94-100 Ma), 4) the tonalitic to granodioritic Needles suite (ca.100-96 Ma), and 5) the granitic Domelands suite (ca. 83-95 Ma). The Kern River suite is the subvolcanic intrusive complex for ca.102-105 Ma Erskine Canyon silicic volcanic-hypabyssal sequence. The Kern River suite is intruded by both the Bear Valley and the Needles suites. These three suites are restricted to the west wall of the proto-Kern Canyon fault (PKCF), a complex ductile shear zone that records both dextral strike-slip and west-directed thrust deformation along the axial zones of the southern SNB. The South Fork and Domelands intrusive suites lie to the east of the PKCF, and the Domelands suite was emplaced incrementally during the principal ductile deformation history of the PKCF.

Age and structural relations indicate that east-side-up ductile thrusting along the PKCF commenced possibly as early as ca.100 Ma, but was clearly operating by ca. 94 Ma, and that dextral shear commenced by ca. 94 Ma. The southern segment of the shear zone and the northern segment are differentiated by the merging of the Kern Canyon fault (KCF) into the PKCF at latitude ~35.7° N. The southern segment of the PKCF exhibits a higher magnitude of crustal shortening by its early phases of thrust displacement. Dextral ductile shear waned along the northern segment of the shear zone by ca. 83 Ma, and terminated by ca. 86 for the southern segment. The prolonged dextral shear along the northern segment relative to the southern segment may signal the inception and shunting of the Kern Canyon fault into the northern segment. Dip-slip components of displacement along the PKCF have resulted in two different paleo-depth gradients in its opposing walls along the southern SNB oblique crustal section.

Regional patterns in pluton emplacement and deformation along the PKCF may be correlated in time to analogous pluton emplacement patterns and deformations of the central SNB. These may be further correlated with deformation and unroofing of the deepest exposed levels of the SNB to the south and the low-angle underthrusting and tectonic underplating of Franciscan subduction accretion assemblages beneath the deep-level rocks. This deformation history is also recorded in the depositional history of the adjacent Great Valley forearc basin, and in some metaclastic units of the southern Franciscan subduction complex.

References

Ague, J. J., 1997, Thermodynamic calculation of emplacement pressures for batholithic rocks, California: implications for the aluminum-in-hornblende barometer: *Geology*, v. 25, p. 563–566.

Ague, J. J., and Brimhall, G. H., 1988, Magmatic arc asymmetry and distribution of anomalous plutonic belts in the batholiths of California: effects of assimilation, crustal thickness, and depth of crystallization: *Geol. Soc. of Amer. Bull.*, v. 100, p. 912–927.

Barth, A. P., Wooden, J. L., Grove, M., Jacobson, C. E., and Pedrick, 2003, U–Pb zircon geochronology of rocks in the Salina Valley region of California: A reevalution of the crustal structure and origin of the Salinian block: *Geology*, v. 31, p. 517–520.

Barton, M. D., and Hanson, R. B., 1989, Magmatism and the development of low-pressure metamorphic belts: implications from the western United States and thermal modeling: *Geol. Soc. Of Amer. Bull*., v. 101, p. 1051–1065.

Bateman, P. C., 1983, A summary of critical relations in the central part of the Sierra Nevada batholith, California, U.S.A.: *Geol. Soc. Of Amer. Mem.,* v. 159, p. 241–254.

Bateman, P. C., and Clark, L. D., 1974, Stratigraphic and structural setting of the Sierra Nevada batholith: *Pacific Geology*, v. 8, p. 79–89.

Bateman, P. C., and Chappell, B. P., 1979, Crystallization, fractionation, and solidification of the Tuolumne intrusive series, Yosemite National Park, California: *Geol. Soc. of Amer. Bull*., v. 90, p. 465–482.

Brown, E.H., and McClelland, 2000, Pluton emplacement by sheeting and vertical ballooning in part of the southwest Coast Plutonic Complex, British Columbia: *Geol. Soc. Amer. Bull.*, v. 112, p. 708–719.

Buddington, A. F., 1959, Granite emplacement with special reference to North America: *Geol. Soc. of Amer. Bull*., v. 70, p. 671–747.

Busby–Spera, C. J., 1984, Large-volume rhyolite ash flow eruptions and submarine caldera collapse in lower Mesozoic Sierra Nevada, California: *Jour. of Geophys. Res.*, v. 89, p. 8417–8427.

Chen, J. H., and Moore, J. G., 1982, Uranium–lead isotopic ages from the Sierra Nevada batholith: *Jour. of Geophys. Res*., v. 87, p. 4761–4784.

Chen, J. H., and Tilton, G. R., 1991, Applications of lead and strontium isotopic relationships to the petrogenesis of granitoid rocks, central Sierra Nevada batholith, California: *Geol. Soc. of Amer. Bull.*, v. 103, p. 439–447.

Clemens–Knott, D., and Saleeby, J. B., 1999, Impinging ring dike complexes in the Sierra Nevada batholith, California: roots of the Early Cretaceous volcanic arc: *Geol. Soc. of Amer. Bull.,* v. 111, n. 4, p. 484–496.

Coleman, D. S., and Glazner, A. F., 1998, The Sierra crest magmatic event: rapid formation of juvenile crust during the Late Cretaceous in California, *in* Ernst, W. G. and Nelson, C. A., eds.: *Integrated Earth and Environment Evolution of the Southwestern United States*, p. 253–272.

Coleman, D. S., Gray, W., and Glazner, A. F., 2004, Rethinking the emplacement and evolution of zoned plutons: geochronologic evidence for incremental assembly of the Tuolumne Intrusive Suite, California: *Geology*, v. 32, p. 433–436.

Dickinson, W., and Snyder, W. S., 1978, Plate tectonics of the Laramide orogeny: *Geol. Soc. of Amer. Mem.,* v. 151, p. 335–366.

Dickinson, W. R., and Gehrels, G. E., 2003, U–Pb ages of detrital zircons from Permian and Jurassic eolian sandstones of the Colorado Plateau, USA: paleogeographic implications: *Sedimentary Geology*, v. 163, p. 29–66.

Dimalanta, C., Taira, A., Yumul, G.P. jr., Tokuyama, H., and Mochizuki, K., 2002, New rates of western Pacific island arc magmatism from seismic and gravity data: *Earth and Planet. Sci. Lett*., v. 202, p. 105–115.

Dixon, E. T., 1995, $^{40}Ar/^{39}Ar$ hornblende geochronology and evaluation of garnet and hornblende barometry, Lake Isabella and the Tehachapi area, southern Sierra Nevada, California: *M.S. thesis*, Univ. of Michigan, 63 pp.

Ducea, M. N., 2001, The California Arc: thick granitic batholiths, ecoglitic residues, lithospheric-scale thrusting, and magmatic flare-ups: *GSA Today*, v. 11, n. 11, p. 4–10.

Ducea, M. N., and Saleeby, J. B., 1996, Buoyancy sources for a large, unrooted mountain range, the Sierra Nevada, California: evidence from xenolith thermobarometry: *Jour. of Geophys. Res.*, v. 101, p. 8,229–8,244.

Ducea, M. N., and Saleeby, J. B., 1998, The age and origin of a thick mafic–ultramafic keel from beneath the Sierra Nevada Batholith: *Contrib. Mineral. Petrol*., v. 133, p. 169–185.

Dunne, G. C., and Saleeby, J. B., 1993, Kern Plateau shear zone, southern Sierra Nevada – new data concerning age and northward continuation: *Geol. Soc. of Amer. Abstr. with Progr.*, v. 25, p. 33.

Dunne, G. C., and Saleeby, J. B., 2006, Structure and geochronology of batholithic and metamorphic framework rocks of the Kern Plateau, southern Sierra Nevada, California: *Geol. Soc. of Amer. Bull.,* in review.

Evernden, J. F., and Kistler, R. W., 1970, Chronology of emplacement of Mesozoic batholithic complexes in California and western Nevada: *U.S. Geol. Surv. Prof. Pap*. 623, 42 pp.

Fliedner, M. M., Klemperer, S. L., and Christensen, N. I., 2000, Three–dimensional seismic model of the Sierra Nevada arc, California, and its implications for crustal and upper mantle composition: *Jour. of Geophys. Res*. v. 105, p. 10,899–10,921.

Fiske, R. S., and Tobisch, O. T., 1978, Paleogeographic significance of volcanic rocks of the Ritter Range pendant, central Sierra Nevada, California, *in* Howell, D. G., and McDougal, K. A., eds.: *Mesozoic paleogeography of the western United States*, Pacific Coast Paleogeography Symposium 2, SEPM Section, p. 209–219.

Fiske, R. S., and Tobisch, O. T., 1994, Middle Cretaceous ash-flow tuff and caldera collapse deposit in the Minarets Caldera, east-central Sierra Nevada, California: *Geol. Soc. of Amer. Bull.,* v. 106, p. 582–593.

Fitch, T. J., 1972, Plate convergence, transcurrent faults, and internal deformation adjacent to southeast Asia and the western Pacific: *Jour. of Geophys. Res*., v. 77, p. 4,432–4,460.

Frost, T. P., and Mahood, C. A., 1987, Field, chemical, and physical constraints on mafic–felsic magma interaction in the Lamarck Granodiorite, Sierra Nevada, California: *Geol. Soc. of Amer. Bull*., v. 99, p. 272–291.

Grove, M., Jacobson, C. E., Barth, A. P., and Vucic, A., 2003, Temporal and spatial trends of Late Cretaceous–early Tertiary underplating of Pelona and related schist beneath southern California and southwestern Arizona: *Geol. Soc. of Amer. Spec. Pap.* 375, p. 381–406.

Hamilton, W., and Meyers, 1967, The nature of batholiths: *U.S. Geol. Survey Prof. Pap.* 554–C.

Hanson, R. B., Saleeby, J. B. and Fates, D. G., 1987, Age and tectonic setting of Mesozoic metavolcanic and metasedimentary rocks, northern White Mountains, California, and origin of the Barcroft Structural Break: *Geology*, v. 15, p. 1,074–1,078.

Helider, C., and Mattox, T. N., 2003, The first two decades of the Pu'u O'o–Kupaianaha eruption: chronology and selected bibliography: *U.S. Geol. Surv. Prof. Pap.* 1676, p. 1–27.

Ingersoll, R. V., 1979, Evolution of the Late Cretaceous forearc basin, northern and central California: *Geol. Soc. of Amer. Bull.,* v. 90, Part I, p. 813–826.

Ingersoll, R. V., 1982, Initiation and evolution of the Great Valley forearc basin of northern and central California, U.S.A., *in* Leggett, J. K., ed., Trench–forearc geology: sedimentation and tectonics on modern and ancient active plate margins: *Geol. Soc. of London Spec. Publ.* 10, p. 459–467.

Jarrard, R. D., 1986, Terrane motion by strike-slip faulting of forearc slivers: *Geology*, v. 14, p. 780–783.

Kay, R. W. and Kay, S.M., 1991, Creation and destruction of the lower continental crust, *Geol. Rundsch*., v. 80, p. 259–270.

Kidder, S., Ducea, M. N., Gehrels, G., Patchett, J., and Vervoort, J., 2003, Tectonic and magmatic development of the Salinian Coast Ridge belt, California: *Tectonics*, v. 22, n. 5, p. 1058, doi:10,1029/2002TC001409.

Kistler, R. W., 1990, Two different types of lithosphere in the Sierra Nevada, California: *Geol. Soc. of Amer. Mem.,* v. 174, p. 271–282.

Kistler, R. W., and Peterman, Z., 1973, Variations in Sr, Rb, K, Na and initial $^{87}Sr/^{86}Sr$ in Mesozoic granitic rocks and intruded wall rocks in central California: *Geol. Soc. of Amer. Bull.*, v. 84, p. 3,489–3,512.

Kistler, R. W., Chappell, B. W., Peck, D. L., and Bateman, P. C., 1986, Isotopic variation in the Tuolumne Intrusive Suite, central Sierra Nevada, California: *Contrib. Min. Pet*., v. 94, p. 205–220.

Kistler, R. W., and Ross, D. C., 1990, A strontium isotopic study of plutons and associated rocks of the southern Sierra Nevada and vicinity, California: *U.S. Geol. Surv. Bull*. 1920, 20 pp.

Klepeis, K. A., Clarke, G. L., and Rushmer, T., 2003, Magma transport and coupling between deformation and magmatism in the continental lithosphere: *GSA Today*, v. 13, p. 4–11.

Kokelaar, B. P., 1982, Fluidization of wet sediments during the emplacement and cooling of various igneous bodies: *Jour. Geol. Soc. of London*, v. 139, p. 21–33.

Krogh, T. E., 1982, Improved accuracy of U–Pb zircon ages by the creation of more concordant systems by an air abrasion technique: *Geochim. et Cosmochim. Acta*, v. 46., p. 637–649.

Lackey, J. S., Valley, J. W, and, Saleeby, J. B., 2005, Supracrustal input to magmas in the deep crust of the Sierra Nevada batholith: evidence from high-δ ^{18}O zircon: *Earth and Planet. Sci. Lett.*, v. 235, p. 315–330.

Lahren, M. M., and Schweickert, R. A., 1989, Proterozoic and Lower Cambrian miogeoclinal rocks of Snow Lake pendant, Yosemite–Emigrant Wilderness, Sierra Nevada, California: evidence for major Early Cretaceous dextral translation: *Geology*, v. 17, p. 156–160.

Lee, C.-T., Yin, Q., Rudnick, R. L., Chesley, J. T., and Jacobsen, S. B., 2000, Re–Os isotopic evidence for pre-Miocene delamination of lithospheric mantle beneath the Sierra Nevada, California: *Science*, v. 289, p. 1,912–1,916.

Ludwig, K. R., 2001, *Users Manual for Isoplot/Ex* (rev. 2.49): A geological toolkit for Microsoft Excel: Berkeley Geochronology Center Spec. Pub. 1a, 56 pp.

Mack, S., Saleeby, J. B. and Farrell, J. E., 1979, Origin and emplacement of the Academy pluton, Fresno County, California: *Geol. Soc. of Amer. Bull.*: Part I, v. 90, p. 321–323; Part II, v. 90, p. 633–694.

Malin, P. E., Goodman, E. D., Henyey, T. L., Li, Y.-G., Okaya, D. A., and Saleeby, J. B., 1995, Significance of seismic reflections beneath a tilted exposure of deep continental crust, Tehachapi Mountains, California: *Jour. of Geophys. Res.*, v. 100, p. 2,069–2,087.

Mansfield, C. F., 1979, Upper Mesozoic subsea fan deposits in the southern Diablo Range, California: record of the Sierra Nevada magmatic arc: *Geol. Soc. of Amer. Bull.*, v. 90, p. 1,025–1,046.

Miller, W. J., and Webb, R. W., 1940, Descriptive geology of the Kernville Quadrangle, California: *Calif. Jour. of Mines and Geol.*, v. 36, p. 343–378.

Pickett, D. A., and Saleeby, J. B., 1993, Thermobarometric constraints on the depth of the exposure and conditions of plutonism and metamorphism at deep levels of the Sierra Nevada batholith, Tehachapi Mountains, California: *Jour. of Geophys. Res.*, v. 98, p. 609–629.

Paterson, S. R., Miller, R. B., Alsleben, H., Whitney, D. L., Valley, P. M., and Hurlow, H., 2006, 40-60 km of exhumation during Late Cretaceous contraction and Paleogene arc-oblique extension, Cascades core, Washington: *Jour. of Struct. Geol.*, in press.

Pickett, D. A., and Saleeby, J. B., 1994, Nd, Sr, and Pb isotopic characteristics of Cretaceous intrusive rocks from deep levels of the Sierra Nevada batholith, Tehachapi Mountains, California: *Contrib. Mineral. Petrol*., v. 118, p. 198–205.

Pitcher, W. S., and Berger, A. R., 1972, The geology of Donegal: a study of granite emplacement and unroofing: Regional Geology Series: New York, Wiley Interscience, 435 pp.

Reid, S. A., and Cox, B. F., 1989, Early Eocene uplift of the southernmost San Joaquin basin, California: *Amer. Assoc. of Geol. Bull*., v. 73, p. 549.

Ross, D. C., 1989, The metamorphic and plutonic rocks of the southernmost Sierra Nevada, California and their tectonic framework: *U.S. Geol. Surv. Prof. Pap.* 1381, 159 pp., 2 plts.

Ross, D. C., 1995, Reconnaissance geologic map of the southern Sierra Nevada, Kern, Tulare, and Inyo Counties, California: *U.S. Geol. Surv. Misc. Invest. Series*, Map I–2295, scale 1:125,000.

Ruppert, S., Fliedner, M. M., and Zandt, G., 1998, Thin crust and active upper mantle beneath the southern Sierra Nevada in the western United States, *Tectonophysics*, v. 286, p. 237–252.

Saleeby, J. B., 1981, Ocean floor accretion and volcanoplutonic arc evolution of the Mesozoic Sierra Nevada, California, *in*, Ernst, W. G., ed.: Rubey Volume on the Geotectonic Development of California, Prentice–Hall, Inc., Englewood Cliffs, New Jersey, p. 132–181.

Saleeby, J. B., 1990, Progress in tectonic and petrogenetic studies in an exposed cross–section of young (~100 Ma) continental crust, southern Sierra Nevada, California, *in*, Salisbury, M. H., ed.: Exposed Cross Sections of the Continental Crust, D. Reidel Publishing Co., Dordrecht, Holland, p. 137–158.

Saleeby, J. B., 2003, Segmentation of the Laramide slab – evidence from the southern Sierra Nevada region: *Geol. Soc. of Amer. Bull*., v. 115, p. 655–668.

Saleeby, J. B., Busby, C., Goodin, W. D. and Sharp, W. D., 1978, Early Mesozoic Paleotectonic–Paleogeographic Reconstruction of the Southern Sierra Nevada Region, California, *in* Howell, D., ed.: Mesozoic Paleogeography of the Western United States: Pacific Section, SEPM, p. 311–336.

Saleeby, J. B. and Sharp, W. D., 1980, Chronology of the structural and petrologic development of the southwest Sierra Nevada Foothills, California: *Geol. Soc. of Amer. Bull.* Part I, v. 91, p. 317–320; Part II, v. 91, p. 1,416–1,535.

Saleeby, J. B. and Busby-Spera, C., 1986, Fieldtrip guide to the metamorphic framework rocks of the Lake Isabella area, southern Sierra Nevada, California, *in* Mesozoic and Cenozoic Structural Evolution of Selected Areas, East-Central California: *Geol. Soc. of Amer. Cordilleran Section Guidebook Volume*, p. 81–94.

Saleeby J. B., Sams, D. B., and Kistler, R. W., 1987, U-Pb zircon, strontium, and oxygen isotopic and geochronological study of the southernmost Sierra Nevada batholith, California: *Jour. of Geophys. Res*., v. 92, p. 10,443–10,446.

Saleeby, J. B., Kistler, R. W., Longiaru, S., Moore, J. G. and Nokleberg, W. J., 1990, Middle Cretaceous silicic metavolcanic rocks in the Kings Canyon area, central Sierra Nevada, California. *in* Anderson, J. L., ed.: The Nature and Origin of Cordilleran Magmatism, Boulder, Colorado, *Geol. Soc. of Amer. Mem*. 174, p. 251–270.

Saleeby, J. B., and Busby, C., 1993, Paleogeographic and tectonic setting of axial and western metamorphic framework rocks of the southern Sierra Nevada, California, *in* Dunne, G., and McDougall, K., eds.: Mesozoic Paleogeography of the Western United States–II: Pacific Section, SEPM, Book 71, p. 197–226.

Saleeby, J. B, Ducea, M. N., and Clemens-Knott, D., 2003, Production and loss of high-density batholithic root–southern Sierra Nevada, California: *Tectonics*, doi:10.1029/2002TC001374.

Saleeby, J. B., Farley, K. A., Kistler, R. W., and Fleck, R., 2006 Thermal evolution and exhumation of deep-level batholithic exposures, southernmost Sierra Nevada, California, *in* Cloos, M., Carlson, W. D., Gilbert, M. C., Liou, J. G., and Sorensen, S. S., eds.: Convergent Margin Terranes and Associated Regions–A Tribute to W.G. Ernst, *Geol. Soc. of Amer. Spec. Pap.* (in press).

Saleeby, J. B., and Zeng, L., 2006, High-magnitude ductile strain in wallrocks during pluton emplacement, southern Sierra Nevada batholith, California: *Tectonics*, in review.

Sisson, T. W., Grove, T. L., and Coleman, D. S., 1996, Hornblende gabbro sill complex at Onion Valley, California, and a mixing origin for the Sierra Nevada batholith: Contrib. Mineral. Petrol., v. 126, p. 81–108.

Skilling, I. P., Busby, C. J., and Imai, T., 2004, Andesitic peperite–bearing debris flows; physical volcanology and paleoenvironment of the Miocene Mehrten Formation, California: *Geol. Soc. of Amer. Abstr. With Prog*., v. 36, n. 4, p. 85.

Stern, T., Bateman, P. C., Morgan, B. A., Newell, M. F., and Peck, D. L., 1981, Isotopic U-Pb ages of zircon from the granitoids of the central Sierra Nevada, California: *U.S. Geol. Surv. Prof. Pap.* 1185, 17 pp.

Terra, F., and Wasserburg, J. G., 1972, U-Pb systematics in lunar basalts: *Earth and Planet. Sci. Lett*., v. 17, p. 65–78.

Tikoff, B. and Teyssier, C., 1992, Crustal-scale, en echelon P–shear tensional bridges – a possible solution to the batholithic room problem: *Geology*, v. 20, p. 927–930.

Tikoff, B. and Saint Blanquat, M., 1997, Transpressional shearing and strike-slip partitioning in the Late Cretaceous Sierra Nevada magmatic arc, California: *Tectonics*, v. 16, p. 442–459.

Tobisch, O. T., Saleeby, J. B., Renne, P. R., McNulty, B., Tong, W., 1995, Variations in the Sierra Nevada, California: *Geol. Soc. of Amer. Bull.*, v. 107, p. 148–166.

Tobisch O. T., Fiske R. S., Saleeby J. B., Holt, E., Sorensen S. S., 2000, Steep tilting of metavolcanic rocks by multiple mechanisms, central Sierra Nevada, California: *Geol. Soc. of Amer. Bull*., v. 112, no. 7, p. 1,043–1,058.

Wong, M.S., 2005, Structural evolution of mid-crustal shear zones: integrated field and thermochronologic studies of the Sierra Mazatán metamorphic core complex, Sonora, Mexico, and the Proto-Kern Canyon dextral shear zone, southern Sierra Nevada, California: *PhD thesis*, University of California, Santa Barbara, 160 pp.

Wood, D. J., and Saleeby, J. B., 1998, Late Cretaceous–Paleocene extensional collapse and disaggregation of the southernmost Sierra Nevada batholith: *Int. Geol. Rev*., v. 39, p. 973–1,009.

Wood, D. J., and Saleeby, J. B., 2006, Structure and geochronology of the eastern Tehachapi Range, southernmost Sierra Nevada batholith, California: *Geol. Soc. of Amer. Bull*., (in review).

Zeng, L., Saleeby, J., and Ducea, M., 2005, Geochemical characteristics of crustal anatexis during the formation of migmatite at the southern Sierra Nevada, California: *Contrib. Min. Pet*., v.150, p. 386–402.

Zeng, L. Ducea, M., and Saleeby, J., 2006, Melting of pelitic sources and the origin of leucogranite dikes in the Isabella pendant, southern Sierra Nevada, California: *Geol. Soc. of Amer. Bull*., in review.

Figure Captions

1. Index map of the southern Sierra Nevada batholith showing location of study area (Fig. 2 box), regional-scale lithologic features, Sr_i=0.706 isopleth (after Kistler, 1990) and, igneous barometric isopleths for the Cretaceous (after Ague and Brimhall, 1988; Pickett and Saleeby, 1993; Ague, 1997; Nadin, Chapter 3).

2. Generalized geologic map of the study area showing intrusive suites and principal defining plutons, and locations of U/Pb zircon samples. Symbols for plutons studied here are defined in Table 1. Geology after Saleeby and Busby-Spera (1986), Ross (1989, 1995) and Nadin (Chapters 4 and 5). Location of Figure 3 geologic map of Erskine Canyon area shown by box.

3. Geologic map of Erskine Canyon area showing relationship between Erskine Canyon sequence and underlying Kings sequence, and the trace of the proto-Kern Canyon fault ductile-brittle damage zone (mapping after Saleeby).

4. Concordia line segments (after Tera and Wasserburg, 1972) stacked in $^{207}Pb/^{206}Pb$ space for concordant or near concordant data error ellipses for samples from the Erskine Canyon sequence and Kern River intrusive suite. Errors are 2 sigma, plotting procedure is modified from Ludwig (2001).

5. Concordia plots and solutions for discordant samples of Erskine Canyon sequence, Kern River and Domelands intrusive suites (after Ludwig, 2001).

6. U/Pb age frequency spectra from laser ablation-ICP-MS data on the Kern River, Bear Valley and Needles intrusive suites (after Ludwig, 2001).

7. Concordia line segments (after Tera and Wasserburg, 1972) stacked in $^{207}Pb/^{206}Pb$ space for concordant or near concordant data error ellipses for samples from the Bear Valley and Needles intrusive suites. Errors are 2 sigma, plotting procedure is modified from Ludwig (2001).

8. Concordia line segments (after Tera and Wasserburg, 1972) stacked in $^{207}Pb/^{206}Pb$ space for concordant or near concordant data error ellipses for samples from the South Fork and Domelands intrusive suites. Errors are 2 sigma, plotting procedure is modified from Ludwig (2001).

9. U/Pb age frequency spectra from laser ablation-ICP-MS data on the South Fork and Domelands intrusive suites.

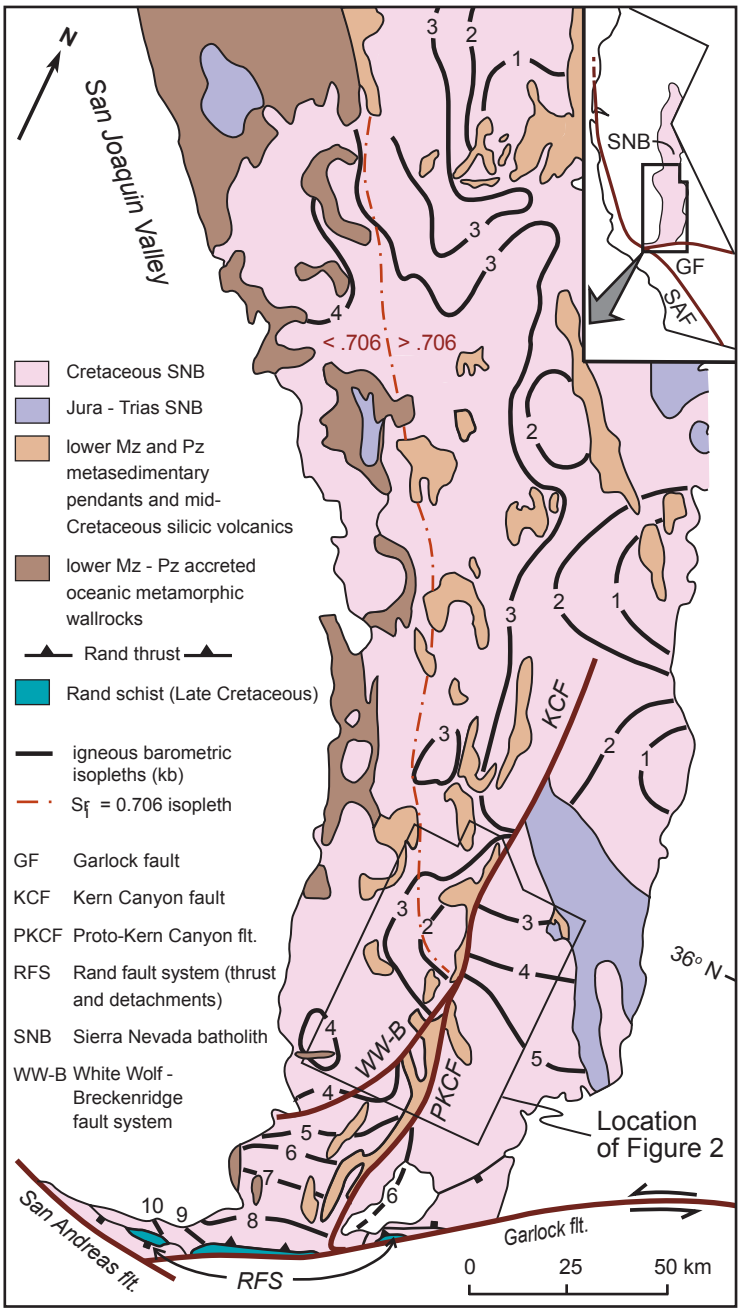
N
San Joaquin Valley
SNB
GF
SAF
< .706
> .706
Cretaceous SNB
Jura - Trias SNB
lower Mz and Pz metasedimentary pendants and mid-Cretaceous silicic volcanics
lower Mz - Pz accreted oceanic metamorphic wallrocks
Rand thrust
Rand schist (Late Cretaceous)
igneous barometric isopleths (kb)
S_i = 0.706 isopleth
GF Garlock fault
KCF Kern Canyon fault
PKCF Proto-Kern Canyon flt.
RFS Rand fault system (thrust and detachments)
SNB Sierra Nevada batholith
WW-B White Wolf - Breckenridge fault system
KCF
WW-B
PKCF
36° N
Location of Figure 2
San Andreas flt.
RFS
Garlock flt.
0
25
50 km

Figure 1

118.75 118.5 118.25

36 35.75 35.5

N

Sample suite symbols

- Domelands suite
- Bear Valley suite
- South Fork suite
- Kern River suite
- Needles suite
- Erskine Canyon sequence

2 0 2 4 6 8 10 mi

2 0 2 4 6 8 10 km

Kne Kpm Kbc Kcr Ksp Kkr Kdm Kpi Klm Kri Kcl Kpp Kcf Kon Kai Kbv Kas Kwf Kbm Kpf Kss Kbo Kma Kce (Kcl) Kcm (Kcl)

Yellowjacket Ridge

Lake Isabella

South Fork Valley

Fig. 3

Walker Basin

Kelso Valley

LEGEND

- Cenozoic sediments and volcanics
- Cretaceous batholithic rocks, nondifferentiated
- Intrusive suite of the Needles, ca. 96 - 100 Ma*
- Intrusive suite of Bear Valley, ca. 98 - 102 Ma*
- Intrusive suite of the Kern River, ca. 102 - 105 Ma*
- Erskine Canyon sequence ca. 102 - 105 Ma silicic volcanic and hypabyssal rocks
- Kings sequence: Jura-Trias quartzite - marble - pelite with Pz metasedimentary basement remnants
- proto- Kern Canyon Fault
- Kern Plateau shear zone intruded out
- Intrusive suite of the Domelands, ca. 95 - 84 Ma*
- Intrusive suite of the South Fork, ca. 94 - 100 Ma*
- Jurassic - Triassic batholithic rocks, nondifferentiated
- El Paso terrane Pz metasediments

Figure 2

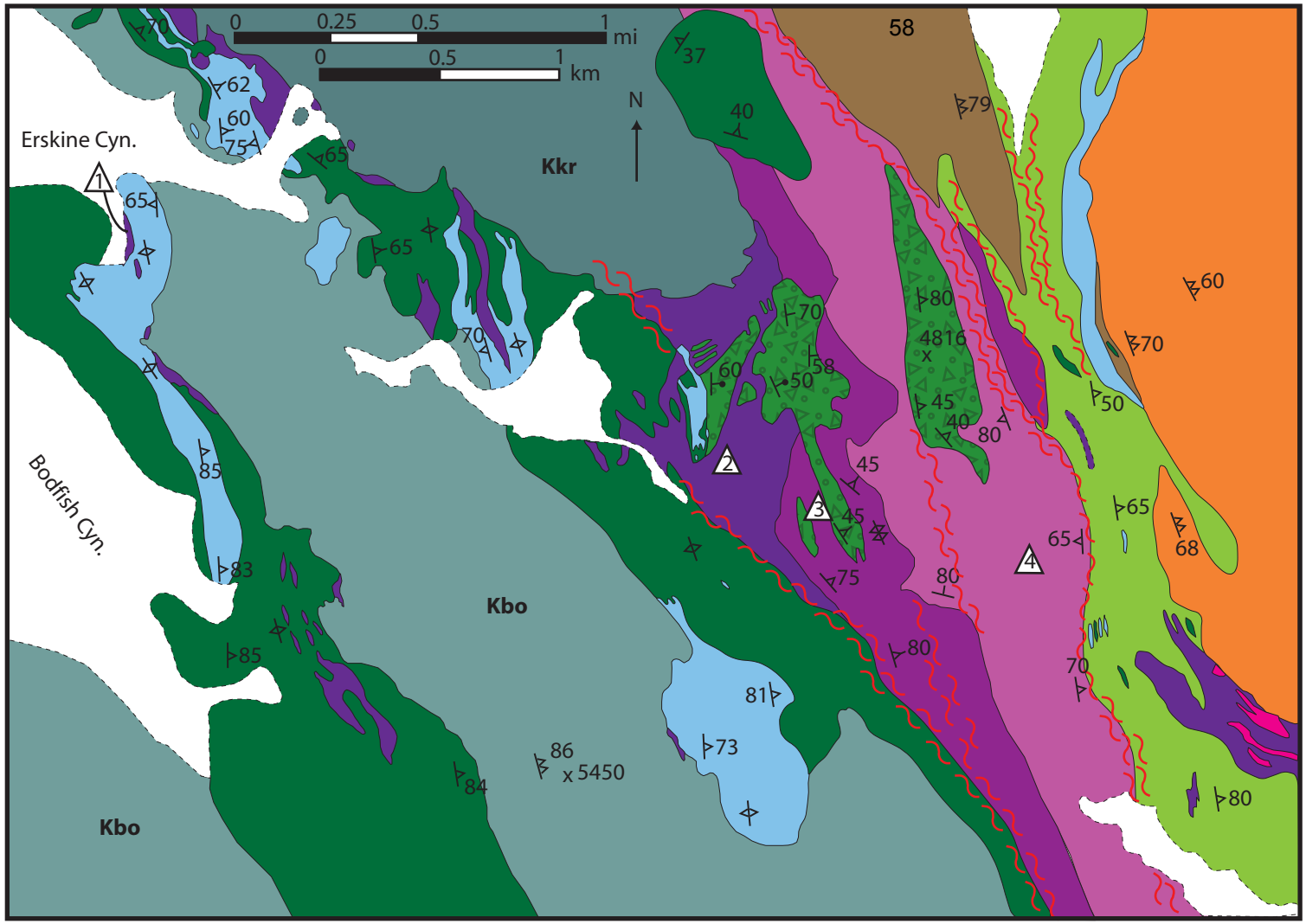

Symbols

- U/Pb zircon sample location
- Ductile-brittle shear zone
- mylonitic foliation
- foliation on crystalloblastic S and L-S fabric
- bedding
- bedding with facing data

LEGEND

- Quaternary alluvium
- Phyllonite and mylonite derived from Kings sequence pendant rocks and Erskine Canyon sequence silicic volcanic and hypabyssal rocks
- Granodiorite of Goat Ranch Canyon (South Fork intrusive suite); ca. 98 Ma
- **Kbo** Granite of Bodfish Canyon (Kern River intrusive suite); ca. 103 Ma
- **Kkr** Granite of the Kern River (Kern River intrusive suite); ca. 105 Ma

Erskine Canyon sequence

- Rhyolitic to dacitic hypabyssal rocks, locally pepperitic adjacent to talus breccia unit; ca. 104 - 105 Ma
- Rhyolitic to dacitic volcanic and volcaniclastic rocks, welded ash flow tuff and subordinate andesite flows, subordinate hypabyssal rocks; ca. 104 Ma
- Mixed rhyolite to andesite volcanic, volcaniclastic rocks including welded ash flow tuff, hypabyssal rocks, and subordinate epiclastic and calc-silicate rocks; ca. 105 Ma
- Epiclastic breccia (talus); quartzite, schist and marble clasts, bedded arenite and subordinate lenses of calc-silicate rocks, marble and tuffaceous grits

Kings sequence

- Quartzite, quartz-mica schist and calc-silicate rock with remnants of bedding
- Banded grey marble
- High-strain schist and gneiss, derived from siliciclastic and calc-silicate rocks

Figure 3

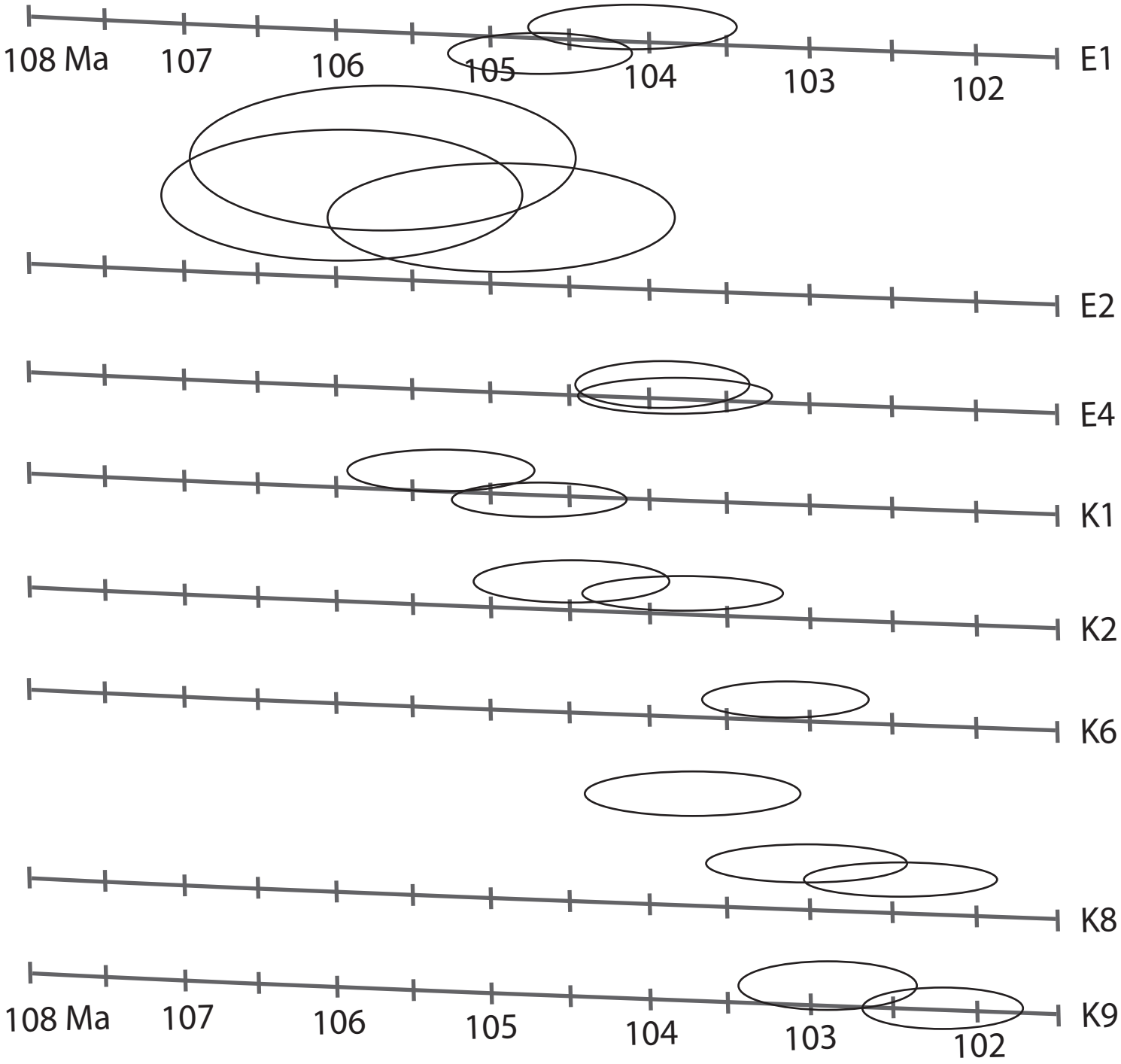
108 Ma
107
106
105
104
103
102
E1
E2
E4
K1
K2
K6
K8
K9
108 Ma
107
106
105
104
103
102

Figure 4

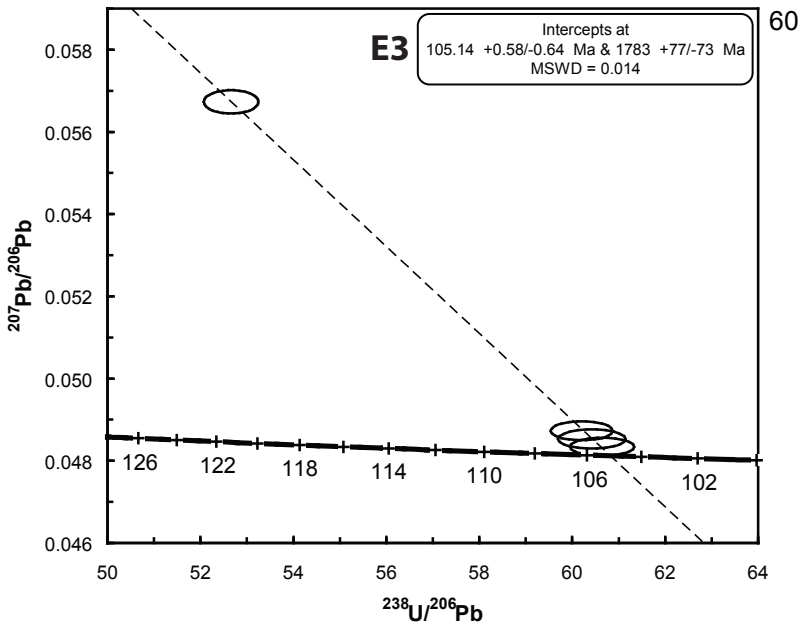
E3
Intercepts at
105.14 +0.58/-0.64 Ma & 1783 +77/-73 Ma
MSWD = 0.014
126
122
118
114
110
106
102
$^{207}Pb/^{206}Pb$
$^{238}U/^{206}Pb$

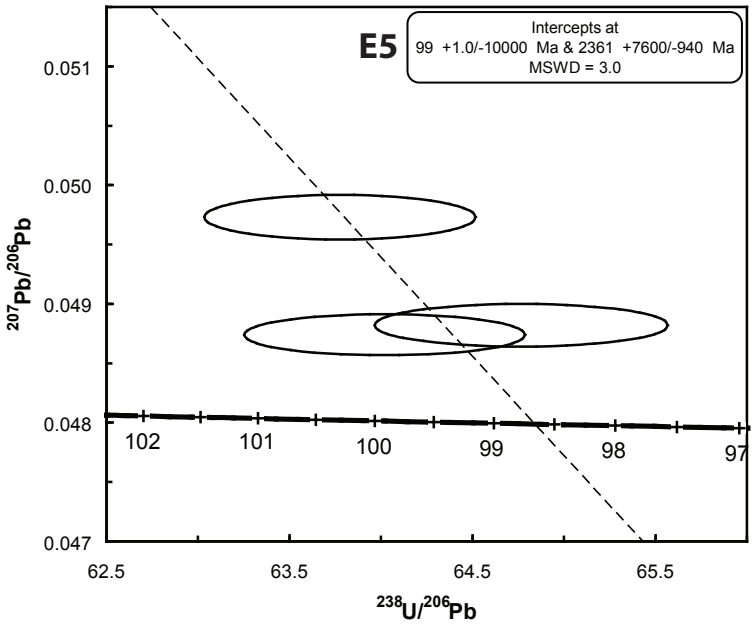
E5
Intercepts at
99 +1.0/-10000 Ma & 2361 +7600/-940 Ma
MSWD = 3.0
102
101
100
99
98
97
$^{207}Pb/^{206}Pb$
$^{238}U/^{206}Pb$

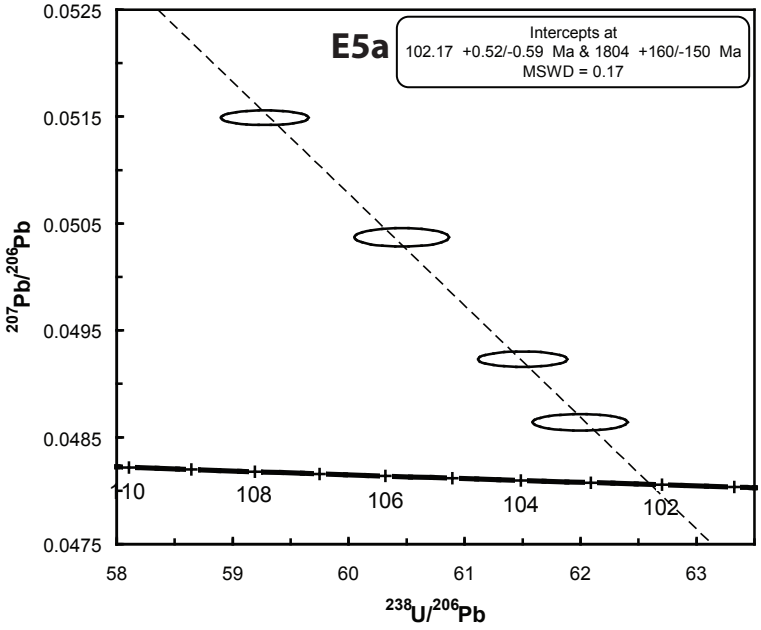
E5a
Intercepts at
102.17 +0.52/-0.59 Ma & 1804 +160/-150 Ma
MSWD = 0.17
110
108
106
104
102
$^{207}Pb/^{206}Pb$
$^{238}U/^{206}Pb$

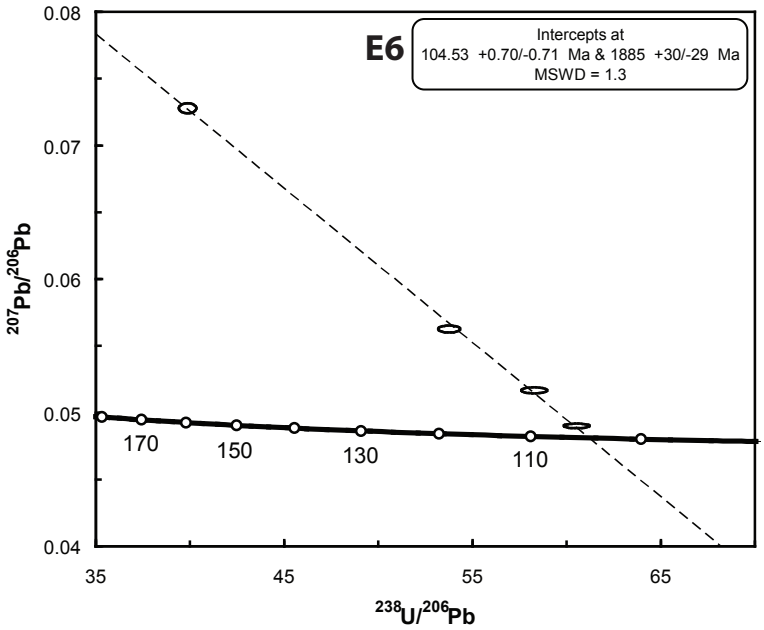
E6
Intercepts at
104.53 +0.70/-0.71 Ma & 1885 +30/-29 Ma
MSWD = 1.3
170
150
130
110
$^{207}Pb/^{206}Pb$
$^{238}U/^{206}Pb$

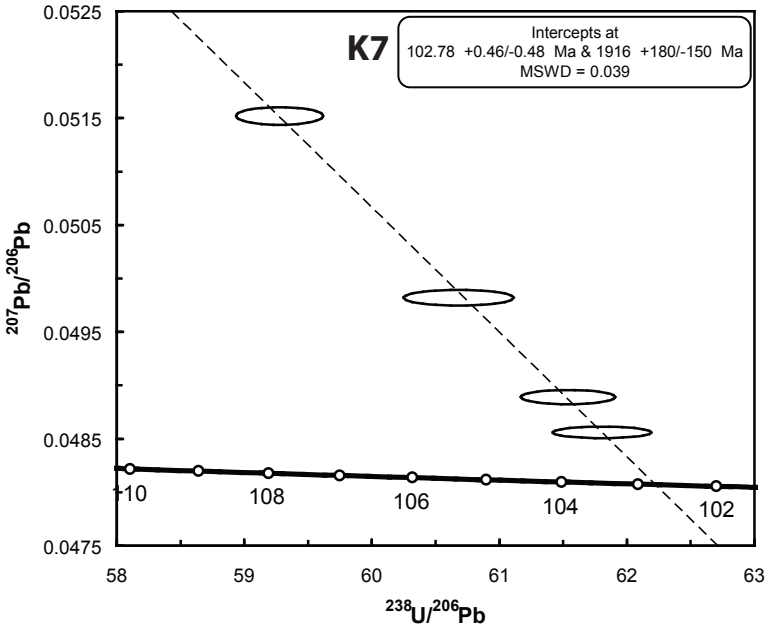
K7
Intercepts at
102.78 +0.46/-0.48 Ma & 1916 +180/-150 Ma
MSWD = 0.039
110
108
106
104
102
$^{207}Pb/^{206}Pb$
$^{238}U/^{206}Pb$

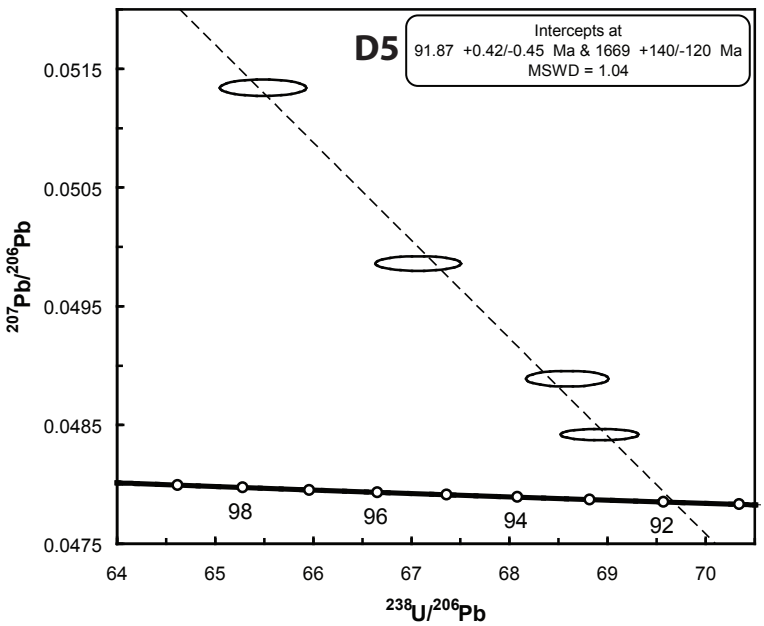
D5
Intercepts at
91.87 +0.42/-0.45 Ma & 1669 +140/-120 Ma
MSWD = 1.04
98
96
94
92
$^{207}Pb/^{206}Pb$
$^{238}U/^{206}Pb$

Figure 5

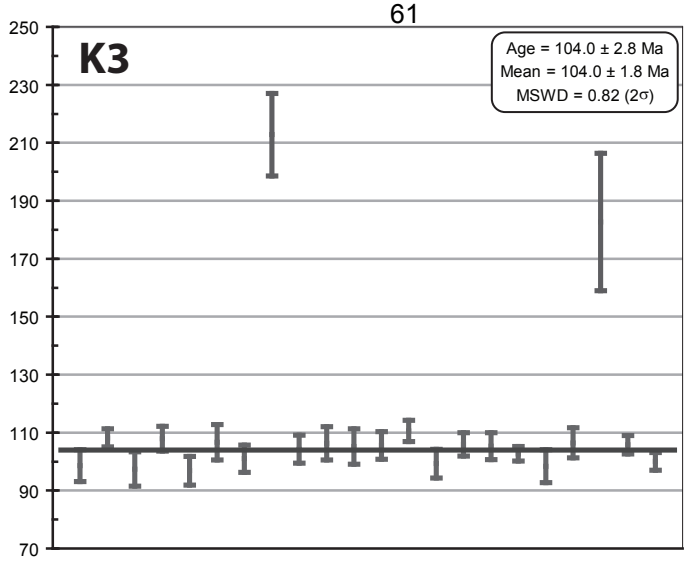
K3
Age = 104.0 ± 2.8 Ma
Mean = 104.0 ± 1.8 Ma
MSWD = 0.82 (2σ)
250
230
210
190
170
150
130
110
90
70

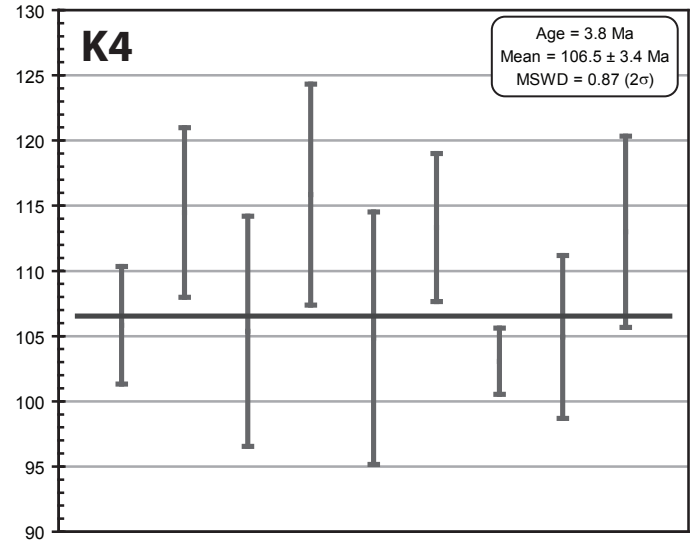
K4
Age = 3.8 Ma
Mean = 106.5 ± 3.4 Ma
MSWD = 0.87 (2σ)
130
125
120
115
110
105
100
95
90

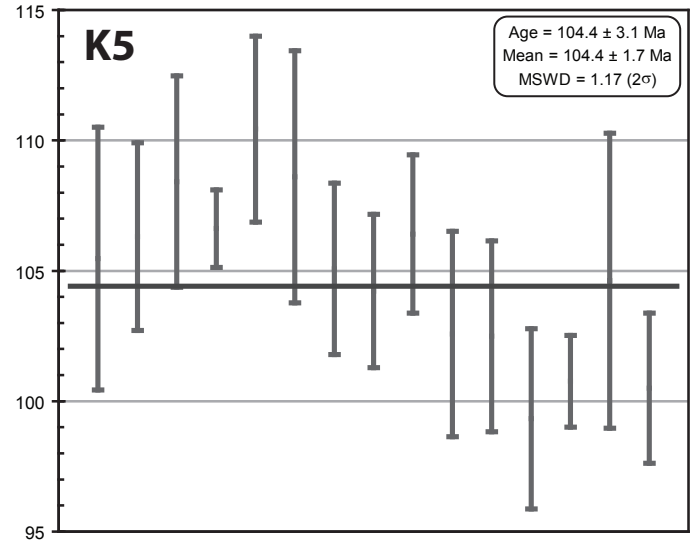
K5
Age = 104.4 ± 3.1 Ma
Mean = 104.4 ± 1.7 Ma
MSWD = 1.17 (2σ)
115
110
105
100
95

Figure 6a

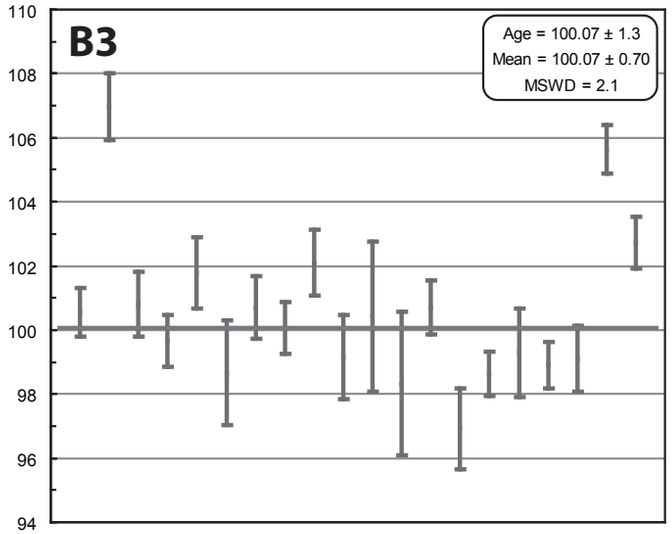
B3
Age = 100.07 ± 1.3
Mean = 100.07 ± 0.70
MSWD = 2.1

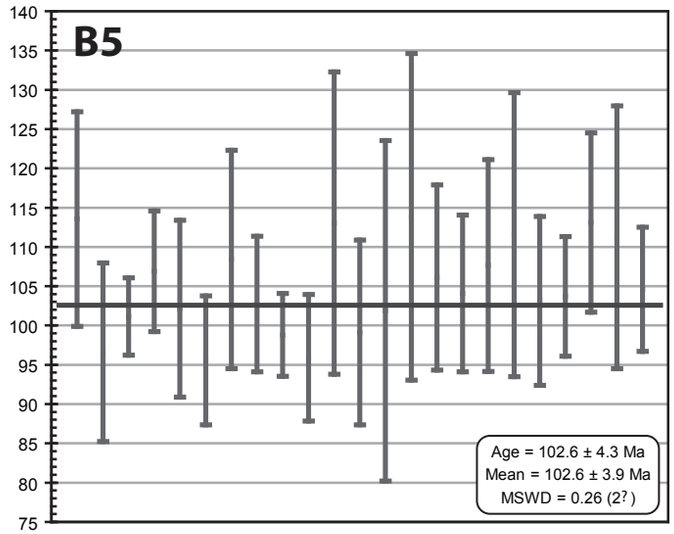
B5
Age = 102.6 ± 4.3 Ma
Mean = 102.6 ± 3.9 Ma
MSWD = 0.26 (2?)

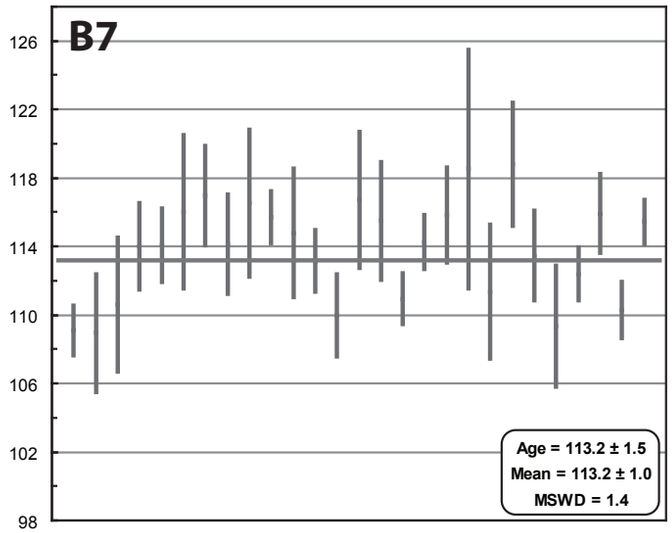
B7
Age = 113.2 ± 1.5
Mean = 113.2 ± 1.0
MSWD = 1.4

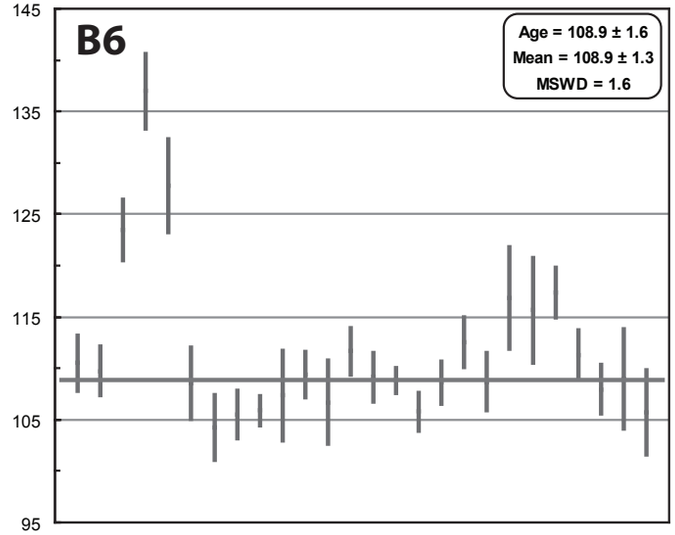
B6
Age = 108.9 ± 1.6
Mean = 108.9 ± 1.3
MSWD = 1.6

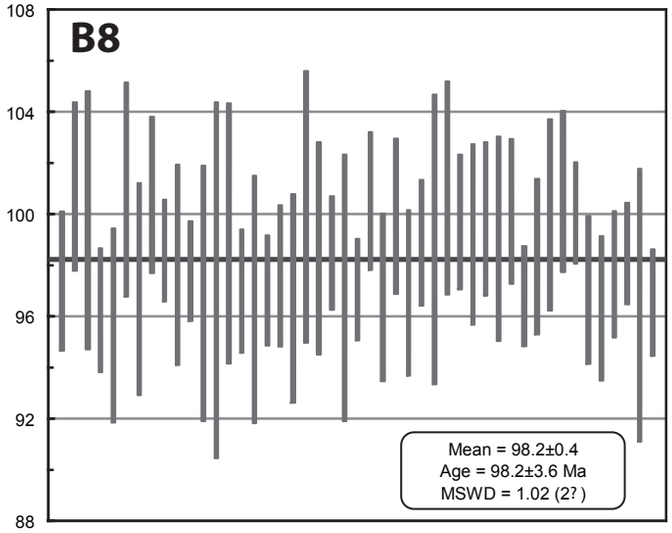
B8
Mean = 98.2±0.4
Age = 98.2±3.6 Ma
MSWD = 1.02 (2?)

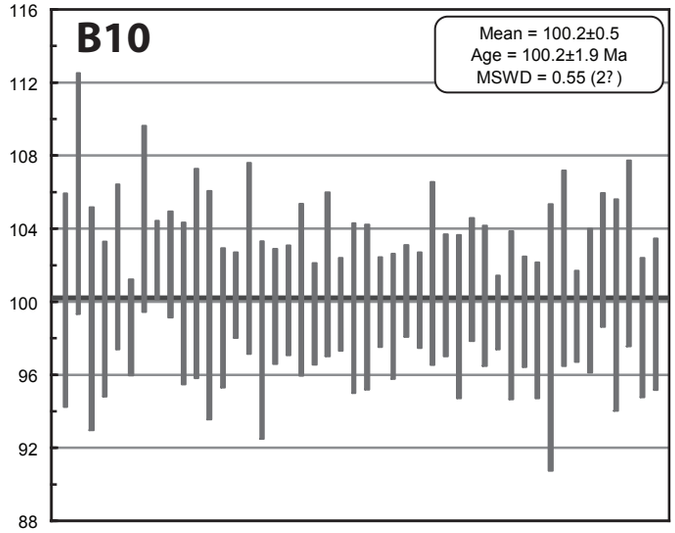
B10
Mean = 100.2±0.5
Age = 100.2±1.9 Ma
MSWD = 0.55 (2?)

Figure 6b

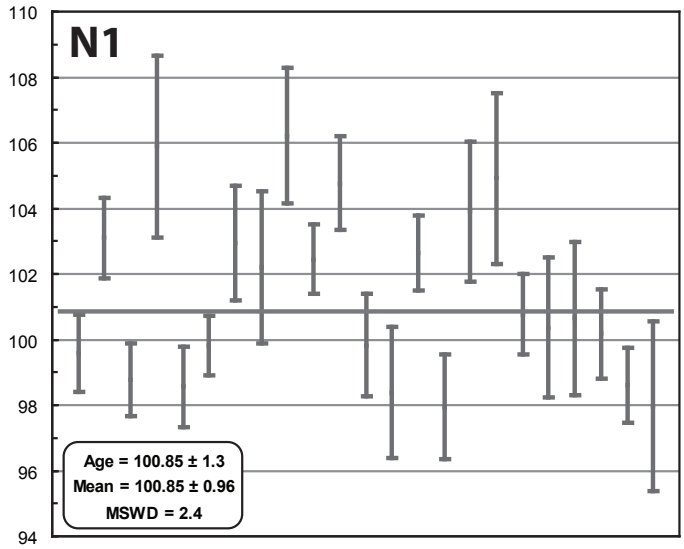

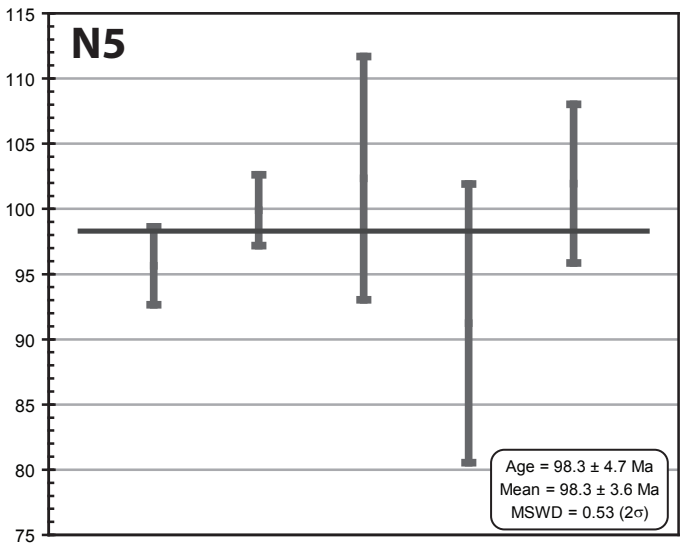

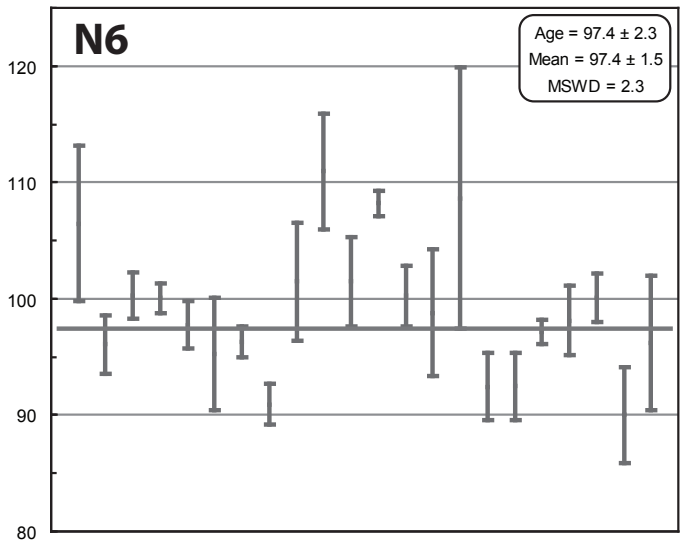

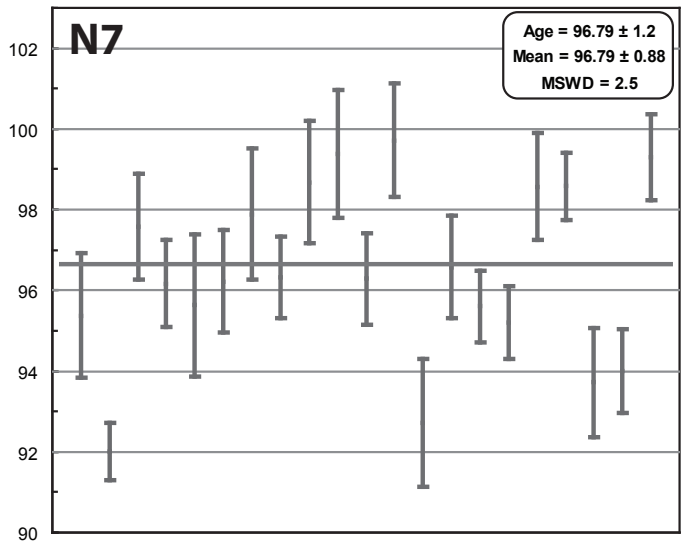

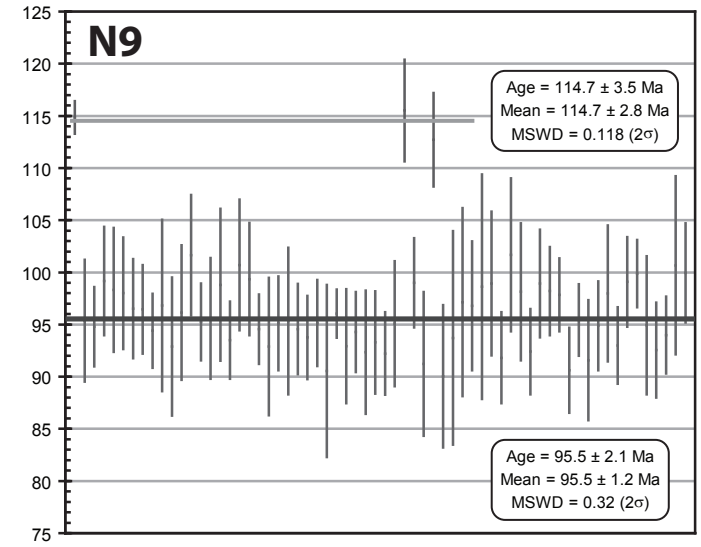

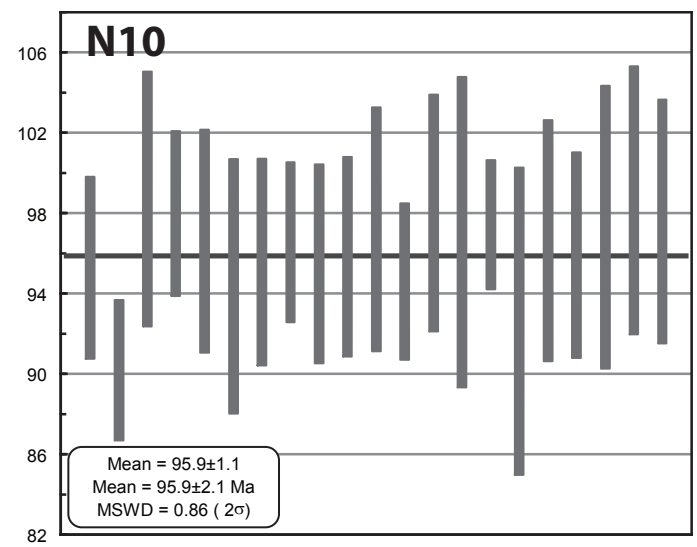

unless specified, errors are 1 sigma

Figure 6c

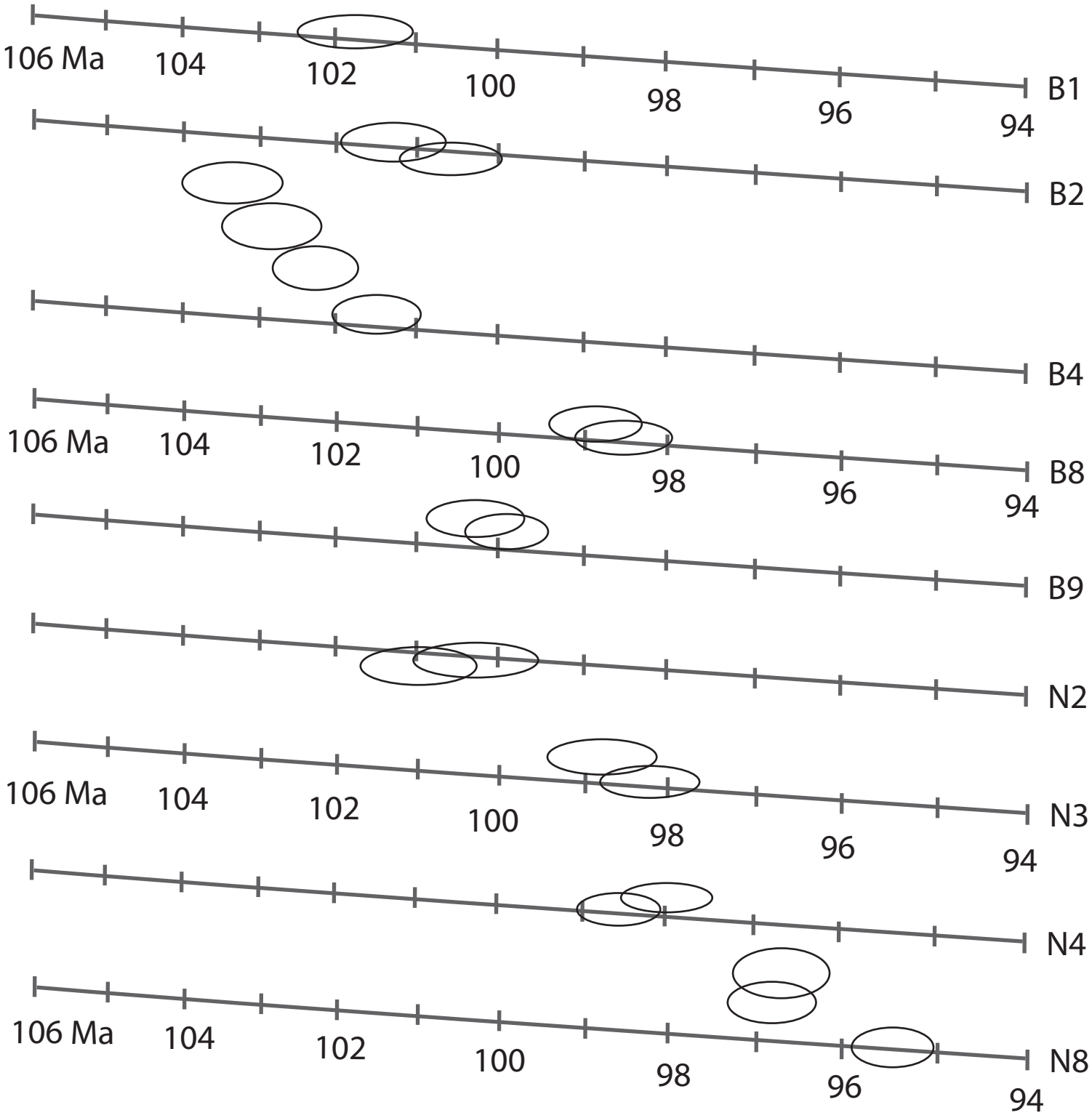

Figure 7

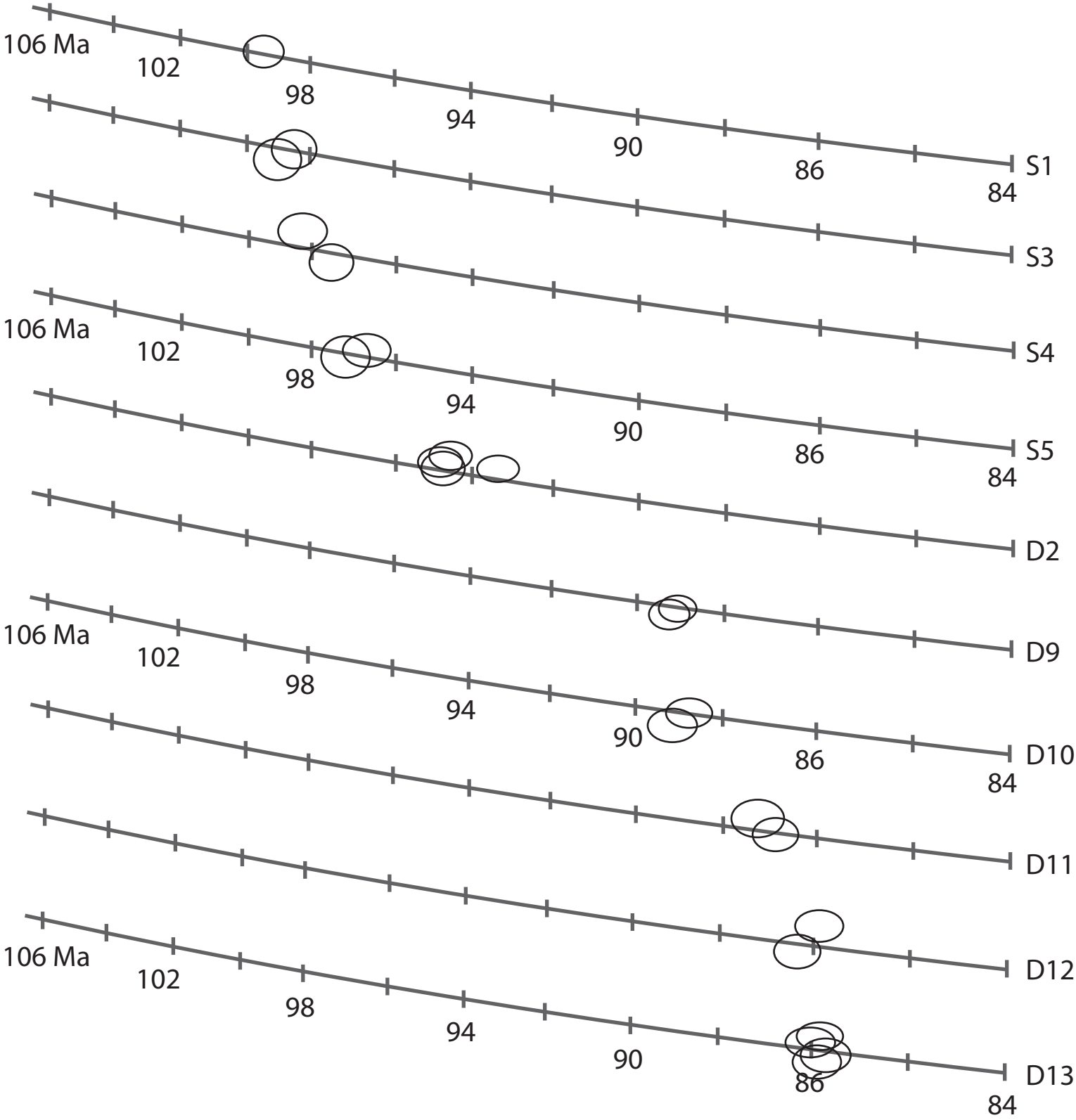

Figure 8

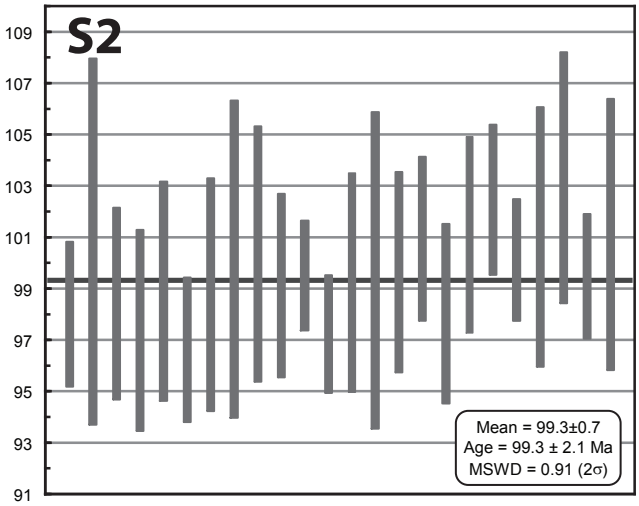
S2
109
107
105
103
101
99
97
95
93
91
Mean = 99.3±0.7
Age = 99.3 ± 2.1 Ma
MSWD = 0.91 (2σ)

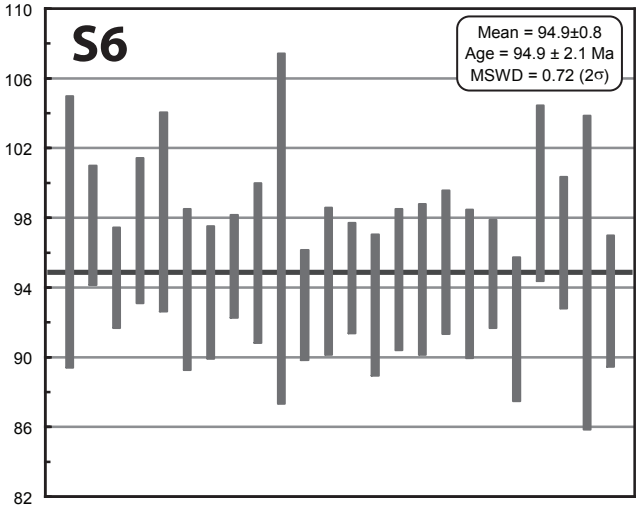
S6
110
106
102
98
94
90
86
82
Mean = 94.9±0.8
Age = 94.9 ± 2.1 Ma
MSWD = 0.72 (2σ)

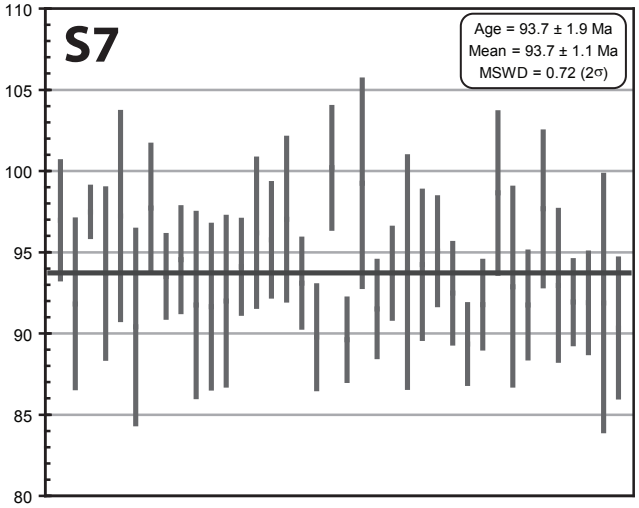
S7
110
105
100
95
90
85
80
Age = 93.7 ± 1.9 Ma
Mean = 93.7 ± 1.1 Ma
MSWD = 0.72 (2σ)

Figure 9a

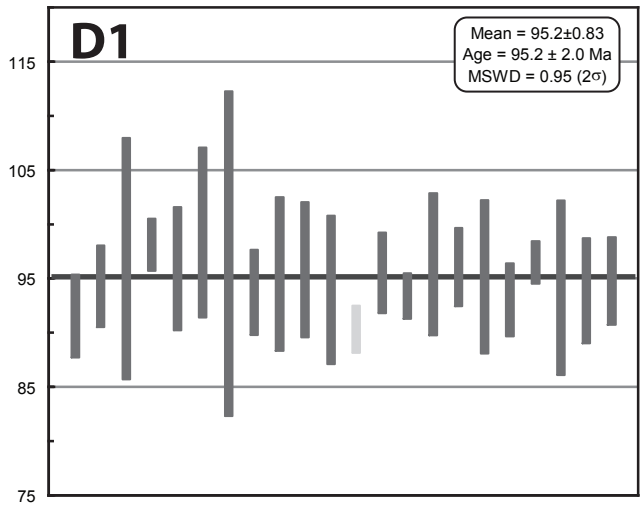
D1
Mean = 95.2±0.83
Age = 95.2 ± 2.0 Ma
MSWD = 0.95 (2σ)
115
105
95
85
75

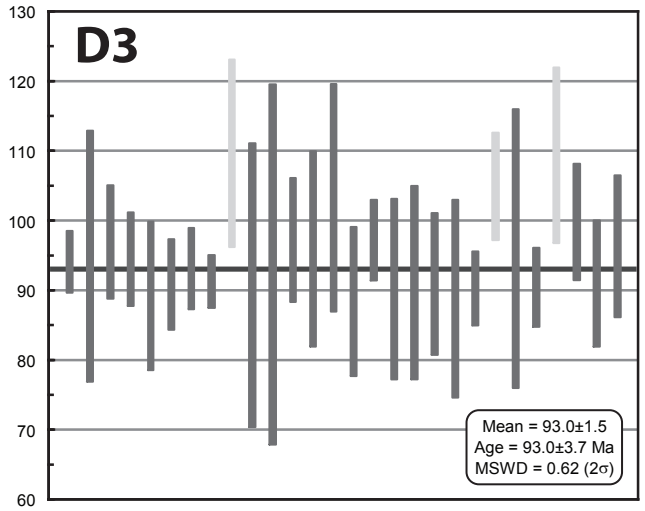
D3
Mean = 93.0±1.5
Age = 93.0±3.7 Ma
MSWD = 0.62 (2σ)
130
120
110
100
90
80
70
60

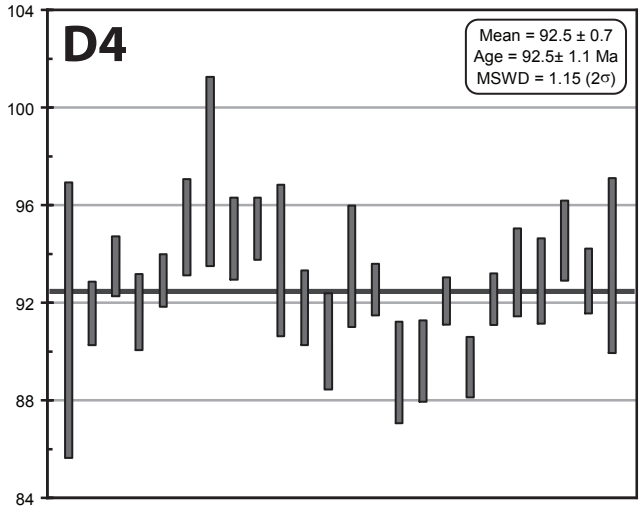
D4
Mean = 92.5 ± 0.7
Age = 92.5± 1.1 Ma
MSWD = 1.15 (2σ)
104
100
96
92
88
84

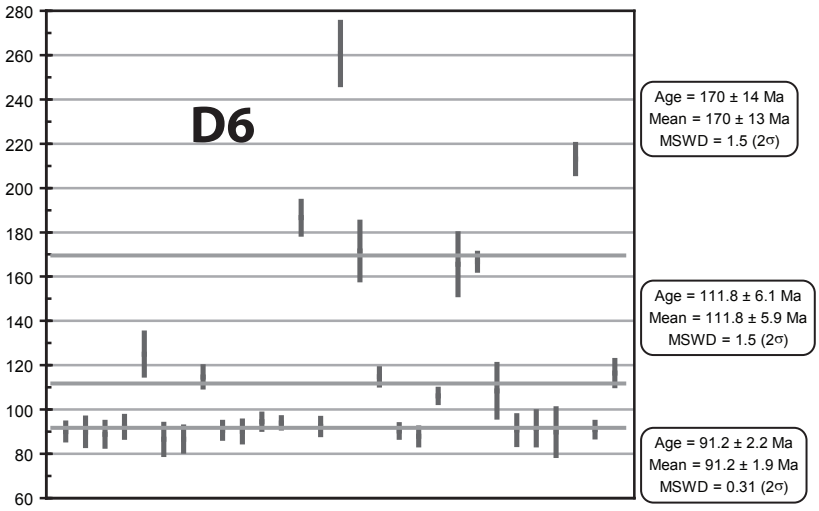
D6
Age = 170 ± 14 Ma
Mean = 170 ± 13 Ma
MSWD = 1.5 (2σ)
Age = 111.8 ± 6.1 Ma
Mean = 111.8 ± 5.9 Ma
MSWD = 1.5 (2σ)
Age = 91.2 ± 2.2 Ma
Mean = 91.2 ± 1.9 Ma
MSWD = 0.31 (2σ)
280
260
240
220
200
180
160
140
120
100
80
60

Figure 9b

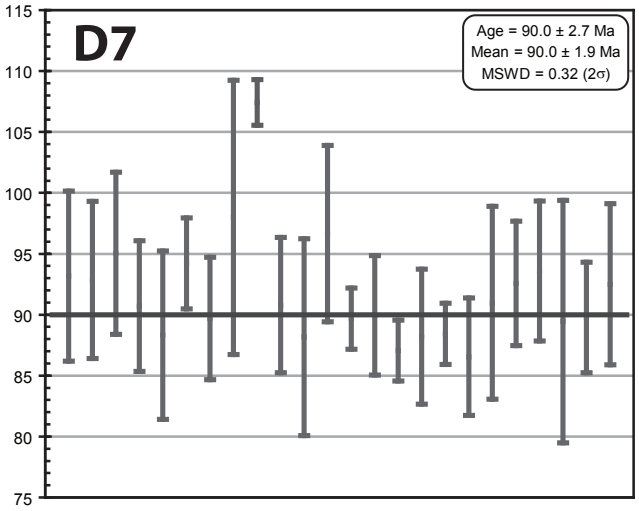
D7
Age = 90.0 ± 2.7 Ma
Mean = 90.0 ± 1.9 Ma
MSWD = 0.32 (2σ)
115
110
105
100
95
90
85
80
75

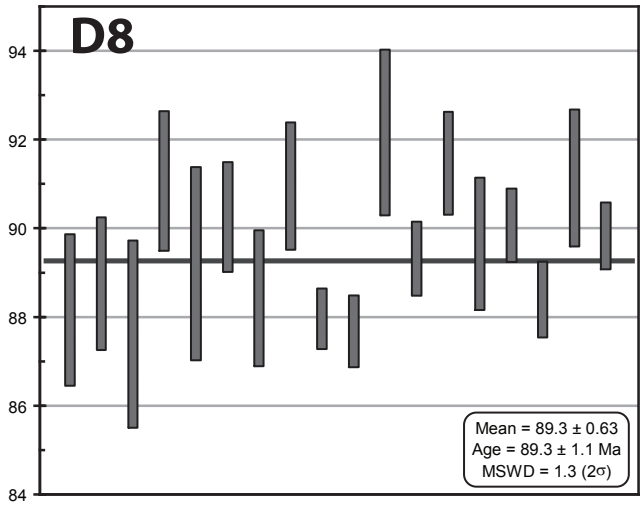
D8
Mean = 89.3 ± 0.63
Age = 89.3 ± 1.1 Ma
MSWD = 1.3 (2σ)
94
92
90
88
86
84

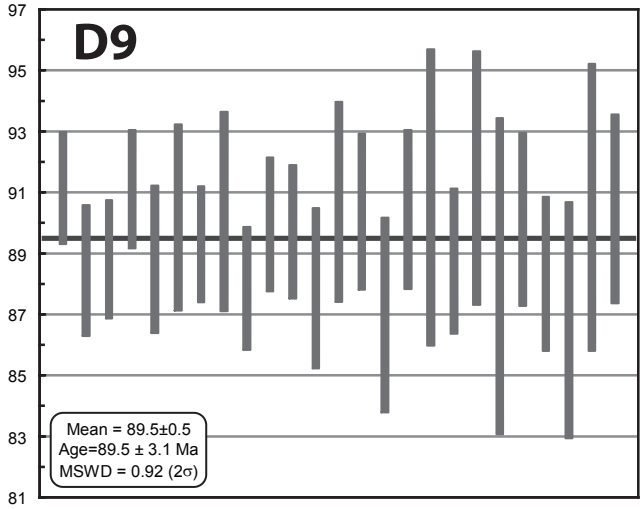
D9
Mean = 89.5±0.5
Age=89.5 ± 3.1 Ma
MSWD = 0.92 (2σ)
97
95
93
91
89
87
85
83
81

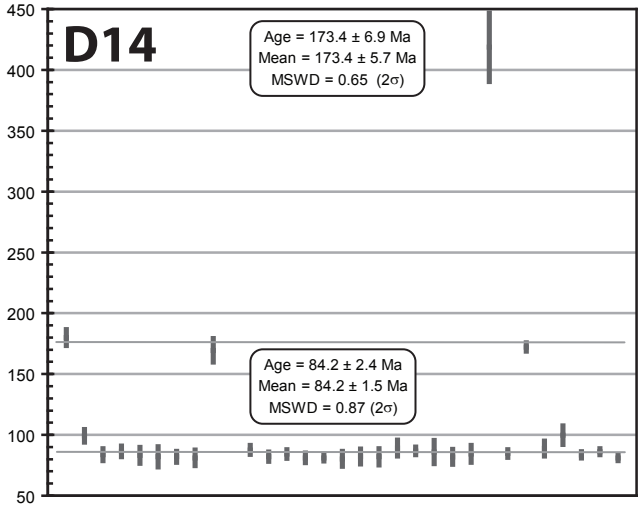
D14
Age = 173.4 ± 6.9 Ma
Mean = 173.4 ± 5.7 Ma
MSWD = 0.65 (2σ)
Age = 84.2 ± 2.4 Ma
Mean = 84.2 ± 1.5 Ma
MSWD = 0.87 (2σ)
450
400
350
300
250
200
150
100
50

Figure 9c

Table 1: Summary of sample locations, nomenclature, petrography, initial $^{87}Sr/^{86}Sr$ (Sr_i) for units dates (after Saleeby et al., 1987; Kistler and Ross, 1990), and U/Pb zircon ages reported here.

Sample Number	Rock Unit	Pluton Map Symbol	Lat°N/Long°W	Petrography	Sr_i	U/Pb Zircon Age (Ma)
Erskine Canyon Sequence						
E1	Hypabyssal intrusion	-	35.592 118.455	Quartz porphyry meta-rhyolite,	-	104.5±0.4
	in Kings sequence			ground mass hornfelsic		
	quartzite-marble					
E2	Pepperitic sill in	-	35.588 118.437	Quartz-alkali feldspar porphyry	-	105.4±0.5
	Kings sequence-			metarhyolite groundmass		
	derived coarse			hornfelsic		
	clastic strata					
E3	Lower ash flow tuff	-	35.589 118.433	Quartz porphry rhyolitic lapilli	-	105.1±0.6
				tuff, flattened pumice lapilli		
				1-10 cm scale, groundmass		
				hornfelsic		
E4	Upper ash flow tuff	-	35.587 118.430	Quartz porphry rhyolitic tuff,	0.70637	104.0±0.3
				fine stretched lapilli groundmass		
				hornfelsic		
E5	Ash flow tuff within	-	35.479 118.632	Tectonitic quartz-feldspar	0.70804	102.2±0.6
	proto-Kern Canyon			porphyry lapilli tuff stretched		
	fault damage zone			pumice lapilli up to 50 cm		
				length, schistose groundmass		
E6	Volcanic neck in	-	35.827 118.443	Plagioclase porphyry dacite	-	104.5±0.7
	Kings sequence			breccia, groundmass hornfelsic		
	quartzites					
Intrusive Suite of the Kern River						
K1	Granite of Kern River	kr	35.875 118.456	K-feldspar-plagioclase-biotite	.70767-0.7081	105.0±0.3
				porphyritic granite with		
				fine-grained groundmass		
K2	Granite of Kern River	"	35.770 118.485	Mildly K-feldspar porphyritic	"	104.3±0.5

Table 1: Summary of sample locations, nomenclature, petrography, initial $^{87}Sr/^{86}Sr$ (Sr_i) for units dates (after Saleeby et al., 1987; Kistler and Ross, 1990), and U/Pb zircon ages reported here.

				granite		
K3	Granite of Kern River	"	35.682 118.443	K-feldspar porphyritic	"	104.0±1.8
				protomylonitic granite		
K4	Granite of Kern River	"	35.615 118.436	K-feldspar porphyritic granite	"	106.5±3.4
K5	Granite of Kern River	"	35.766 118.409	K-feldspar porphyroclastic	-	104.4±1.7
	lens in proto-Kern			mylonitic granite		
	Canyon fault damage					
	zone					
K6	Granite of Portugese	pp	35.787 118.570	Coarse-grained biotite granite	.70852-0.7150	103.2±0.8
	Pass					
K7	Granite of Bodfish	bo	35.527 118.425	Coarse-grained biotite granite	0.70896	102.8±0.5
	Canyon					
K8	Granite of Saddle	ss	35.498 118.399	Medium-grained hornblende	.70608-0.7067	102.5±0.5
	Springs Road-mafic			biotite diorite comingled with		
	phase			granite		
K9	Granite of Baker Point	bp	35.825 118.462	Dacitic porphyry dike rock, fine		103.1±0.9
				biotite and alkali feldspar		
				phenocrysts		
Intrusive Suite of Bear Valley						
B1	Mafic intrusives co-	bm	35.478 118.733	Medium-grained hornblende	-	101.8±0.4
	mingled with Tonalite			diorite		
	of Bear Valley Springs					
B2	Tonalite of Bear	bv	35.507 118.687	Hornblende-biotite tonalite,	0.70430	101.0±0.3
	Valley Springs			uncharacteristically poor in		
				mafic enclaves		
B3	"	"	35.351 118.571	Foliated hornblende-biotite	0.70511	100.1±0.7
				tonalite, rich in flattened		
				mafic inclusions		

Table 1: Summary of sample locations, nomenclature, petrography, initial $^{87}Sr/^{86}Sr$ (Sr_i) for units dates (after Saleeby et al., 1987; Kistler and Ross, 1990), and U/Pb zircon ages reported here.

B4	"	"	35.395 118.435	Foliated-biotite hornblende	0.70425	101.5±0.4
				tonalite, rich in flattened		
				mafic enclaves		
B5	"	"	35.750 118.585	Coarse-grained mafic biotite	0.70576	102.6±3.9
				tonalite		
B6	Early Cretaceous	-	35.436 118.517	Foliated biotite tonalite	-	108.9±1.3
	tonalite enclave within			with sparce mafic enclaves		
	Tonalite of Bear Valley					
	Springs					
B7	Early Cretaceous	-	35.451 118.589	Hornblende-biotite tonalite	-	113.2±1.0
	tonalite gneiss enclave			gneiss		
	within Tonalite of Bear					
	Valley Springs					
B8	Tonalite of Mount	ma	35.454 118.734	Coarse grained biotite	0.70449	98.4±0.2
	Adelaide			tonalite with sparce mafic		
				inclusions		
B9	Granodiorite of Poso Fla	pf	35.575 118.566	Coarse-grained biotite	0.70478	100.1±0.3
				tonalite with sparce mafic		
				inclusions		
B10	Granodiorite of Poso Fla	"	35.603 118.648	Coarse-grained biotite	0.70490	100.2±0.5
				granodiorite poor in mafic		
				inclusions		
Intrusive Suite of the Needles						
N1	Granodiorite of	al	35.666 118.588	Medium-grained hornblende-	.70638-0.7067	100.9±1.0
	Alder Creek			biotite granodiorite		
N2	Granodiorite of	bc	35.975 118.473	Mafic hornblende granodiorite	0.70625	100.6±0.4
	Brush Creek			with abundant mafic inclusions		
N3	Tonalite of Dunlap	dm	35.826 118.600	Medium-grained hornblende-	.70658-0.7071	98.5±0.5
	Meadow			biotite tonalite		

Table 1: Summary of sample locations, nomenclature, petrography, initial $^{87}Sr/^{86}Sr$ (Sr_i) for units dates (after Saleeby et al., 1987; Kistler and Ross, 1990), and U/Pb zircon ages reported here.

N4	Granodiorite of	pi	35.852 118.626	Medium-grained hornblende-	.70669-0.7074	98.3±0.4
	Pine Flat			biotite granodiorite		
N5	Granodiorite of	as	35.669 118.486	Fine- grained biotite porphyritic	.70616-0.7065	98.3±3.6
	Alta Sierra			granodiorite		
N6	Granodiorite of	pm	35.976 118.569	Medium-grained hornblende-	0.70616	97.4±1.5
	Peppermint Meadow			biotite granodiorite		
N7	Granodiorite of the	ne	36.095 118.463	Hornblende-biotite granodiorite	-	96.8±0.7
	Needles			with ductile deformation fabric		
N8	"	"	35.105 118.487	Hornblende-biotite granodiorite	-	96.0±0.5
N9	Granodiorite of	wf	35.676 118.464	Coarse-grained biotite	.70649-0.7068	95.5±1.2
	Wagy Flat			granodiorite		
N10	"	"	35.426 118.420	Coarse-grained biotite	"	95.9±1.1
				granodiorite		
Intrusive Suite of the South Fork						
S1	Quartz diorite of	cf	35.717 118.406	Poikiolitic hornblende-	0.70677	99.6±0.3
	Cyrus Flat			hypersthene leucogabbro		
S2	Alaskite of Sherman	sp	35.982 118.359	Coarse-grained hornblende-	-	99.3±0.7
	Pass			biotite leucogranodiorite		
S3	Granodiorite of	ri	35.673 118.353	Medium-grained hornblende-	.70593-0.7079	99.0±0.4
	Rabbit Island			biotite granodiorite, abundant		
				mafic inclusions		
S4	"	"	35.615 118.249	Medium-grained hornblende-	"	98.1±0.3
				biotite granodiorite, common		
				mafic inclusions		
S5	"	"	35.578 118.393	Medium-grained hornblende-	"	97.0±0.4
				biotite granodiorite, ductile		

Table 1: Summary of sample locations, nomenclature, petrography, initial $^{87}Sr/^{86}Sr$ (Sr_i) for units dates (after Saleeby et al., 1987; Kistler and Ross, 1990), and U/Pb zircon ages reported here.

				deformation fabric and stretched		
				mafic inclusions		
S6	"	"	35.563 118.147	Coarse-grained hornblende-	"	94.9±0.8
				biotite granodiorite, common -		
				mafic inclusions		
S7	"	"	35.729 118.376	Medium-grained hornblende-	"	93.7±1.1
				biotite granodiorite, ductile		
				deformation fabric		
Intrusive Suite of the Domelands						
D1	Granite of Long	lm	35.848 118.349	Medium-grained biotite granodiorite	-	95.2±0.8
	Meadow					
D2	Granite of Cannell	cc	35.709 118.416	Biotite granodiorite	0.70725-	94.7±0.4
	Creek			mylonite	0.70930	
D3	Granite of Onyx	on	35.701 118.235	Fine-grained biotite-bearing granite	0.70801	93.0±1.5
D4	Granodiorite of	cl	35.462 118.281	K-feldspar porphyritic	0.70751	92.5±0.7
	Claraville			biotite granodiorite	0.70800	
D5	Grandiorite of Claraville	ce	35.380 118.342	Medium-grained biotite granodiorite-	0.70704-	91.7±0.8
	(equigranular facies)			modest planar ductile deformation	0.70766	
				fabric		
D6	Grandiorite of Claraville	cl	35.741 118.143	K-feldspar porphyritic biotite	0.70706	91.2±1.9
				granodiorite		
D7	"	"	35.791 118.050	Medium-grained biotite granodiorite	-	90.0±1.9
D8	Granodiorite of	cm	34.483 118.227	Medium-grained hornblende-biotite	-	89.3±0.6
	Claraville (dark facies)			granodiorite		
D9	Granite of Castle Rock	cr	35.986 118.443	K-feldspar megacrystic biotite	0.70762	89.3±0.2

Table 1: Summary of sample locations, nomenclature, petrography, initial $^{87}Sr/^{86}Sr$ (Sr_i) for units dates (after Saleeby et al., 1987; Kistler and Ross, 1990), and U/Pb zircon ages reported here.

				granodiorite protomylontic		
D10	"	"	35.744 118.309	Meduim-grained biotite-granodiorite	-	89.0±0.5
D11	"	"	35.857 118.407	Megacrystic K-feldspar biotite	-	87.1±0.4
				granodiorite, mild ductile		
				deformation fabric		
D12	Granodiorite of	-	35.444 118.370	Leucogranite pegmatite	-	86.1±0.4
	Claraville, isolated					
	leucogranite dike					
D13	Granite of Castle	-	35.801 118.416	Leucogranite pegmatite mylonite	-	85.7±0.5
	Rock, pegmetite dike					
	swarm					
D14	Granite of Castle	cd	35.736 118.077	Medium-grained biotite leucogranite	-	84.2±1.5
	Rock, leucogranite					
	dike swarm					